Developmental Biology 334 (2009) 119–132

Contents lists available at ScienceDirect

Developmental Biology

journal homepage: www.elsevier.com/developmentalbiology

VEGF-A and Semaphorin3A: Modulators of vascular sympathetic innervation

Jennifer B. Long [a], Steven M. Jay [b], Steven S. Segal [d], Joseph A. Madri [c,*]

[a] Department of Cellular and Molecular Physiology, Yale University School of Medicine, New Haven, Connecticut, USA
[b] Department of Biomedical Engineering, Yale University School of Medicine, New Haven, CT 06520, USA
[c] Department of Pathology, Yale University School of Medicine, P.O. Box 208023, New Haven, Connecticut, USA
[d] Department of Medical Pharmacology and Physiology, Dalton Cardiovascular Research Center, University of Missouri, Columbia, Missouri, USA

ARTICLE INFO

Article history:
Received for publication 12 January 2009
Revised 29 June 2009
Accepted 9 July 2009
Available online 23 July 2009

Keywords:
Sympathetic innervation
Vascular endothelial growth factor-A
Semaphorin3A
Neuropilin-1
Superior cervical ganglion
Femoral artery
Carotid artery

ABSTRACT

Sympathetic nerve activity regulates blood pressure by altering peripheral vascular resistance. Variations in vascular sympathetic innervation suggest that vascular-derived cues promote selective innervation of particular vessels during development. As axons extend towards peripheral targets, they migrate along arterial networks following gradients of guidance cues. Collective ratios of these gradients may determine whether axons grow towards and innervate vessels or continue past non-innervated vessels towards peripheral targets. Utilizing directed neurite outgrowth in a three-dimensional (3D) co-culture, we observed increased axon growth from superior cervical ganglion explants (SCG) towards innervated compared to non-innervated vessels, mediated in part by vascular endothelial growth factor (VEGF-A) and Semaphorin3A (Sema3A) which both signal via neuropilin-1 (Nrp1). Exogenous VEGF-A, delivered by high-expressing VEGF-A–LacZ vessels or by rhVEGF-A/alginate spheres, increased sympathetic neurite outgrowth while exogenous rhSema3A/Fc decreased neurite outgrowth. VEGF-A expression is similar between the innervated and non-innervated vessels examined. Sema3A expression is higher in non-innervated vessels. Spatial gradients of Sema3A and VEGF-A may promote differential Nrp1 binding. Vessels expressing high levels of Sema3A favor Nrp1-PlexinA1 signaling, producing chemorepulsive cues limiting sympathetic neurite outgrowth and vascular innervation; while low Sema3A expressing vessels favor Nrp1-VEGFR2 signaling providing chemoattractive cues for sympathetic neurite outgrowth and vascular innervation.

Introduction

Sympathetic regulation of blood pressure maintains cardiovascular homeostasis and responsiveness to physical stress. Major feed arteries and precapillary arterioles are innervated, whereas capillaries, venules and collecting veins are sparsely innervated (Birch et al., 2008; Fleming et al., 1989; Grasby et al., 1999; Ruffolo et al., 1991; Tan et al., 2007). Variations in vascular sympathetic innervation suggest that vascular-derived guidance cues expressed during development determine patterns of innervation.

Axon extension from developing sympathetic neurons often follows arterial networks towards more peripheral targets (Glebova and Ginty, 2005) but little is known about how vessels themselves are selected as targets for innervation. Axon outgrowth and target innervation are governed by gradients of guidance cues that can be local, long-range, contact-mediated, secreted, attractive or repulsive (Tessier-Lavigne and Goodman, 1996). Guidance cues include growth factors, extracellular matrix molecules and “classical” axon guidance molecules (netrins, slits, semaphorins, and ephrins) (Young et al., 2004). Disruption of single signaling pathways results in complex inhibitory profiles suggesting that multiple molecules govern innervation patterns (Belliveau et al., 1997; Glebova and Ginty, 2004; Kuruvilla et al., 2004). Vascular cells express neurotrophins and axon guidance molecules, known to affect vascular morphogenesis and angiogenesis as well as axon outgrowth and guidance (Adams et al., 1999; Carmeliet, 2003; Enomoto et al., 2001; Herzog et al., 2001; Honma et al., 2002).

Angiogenic factors exert neurotrophic and neuroprotective effects in-vivo and in-vitro (Cheng et al., 2004; Rosenstein and Krum, 2004; Schwarz et al., 2004; Sondell and Kanje, 2001; Sondell et al., 1999; Sondell et al., 2000; Storkebaum et al., 2005; Wingerd et al., 2002). VEGF-A promotes axon outgrowth and neuronal survival in-vitro by paracrine and autocrine pathways in dorsal root ganglion (DRG) and SCG via flk-1 (VEGFR2) signaling (Ogunshola et al., 2002; Lin et al., 2003; Sondell and Kanje, 2001) and has been shown to modulate sympathetic growth cone collapse and spreading and promote re-innervation following local nerve damage (Damon, 2006; Marko and Damon, 2008).

Nrp1, a co-receptor for VEGFR2, is implicated in VEGF-A signaling (Soker et al., 1998) and is also a receptor for Sema3A, a chemorepulsive factor that causes growth cone collapse and axon repulsion and has been implicated in modulating vascular sympathetic innervation (Fan and Raper, 1995; He and Tessier-Lavigne, 1997;

* Corresponding author. Fax: +1 203 785 7213.
E-mail address: joseph.madri@yale.edu (J.A. Madri).

0012-1606/$ – see front matter © 2009 Published by Elsevier Inc.
doi:10.1016/j.ydbio.2009.07.023

Kolodkin et al., 1997). Sema3A or Nrp1 inactivation causes decreased peripheral target innervation (Kitsukawa et al., 1997). While previous in-vitro studies suggested competitive binding of Nrp1 by VEGF-A and Sema3A (Appleton et al., 2007; Geretti et al., 2008; Miao et al., 1999), more recent in-vivo data suggests that this may not be the case. Instead, in-vivo, VEGF-A and Sema3A may direct vessel and axon growth in a context dependent manner, which is determined by the localization or concentration of these Nrp1 ligands in a given environment (Schwarz et al., 2004; Vieira et al., 2007). For example, in the facial nerve, Sema3A is required for proper pathfinding of facial motor axons while VEGF-A is required for the proper migration of their somata (Schwarz et al., 2004). In neural progenitor cells, both VEGF-A and Sema3A reciprocally antagonize the opposing signaling pathway, suggesting that their relative concentrations may determine cellular behaviors including migration, proliferation and apoptosis (Bagnard et al., 2001). Thus, both vessel-derived VEGF-A and Sema3A may influence sympathetic innervation patterning depending on specific ligand–receptor interactions.

Here, we evaluate directed sympathetic neurite outgrowth towards innervated and non-innervated vessels in an in-vitro 3D co-culture system. We hypothesize that both VEGF-A and Sema3A drive selective sympathetic neurite outgrowth and may play a role in determining vascular innervation during development. Our results suggest that vascular-derived VEGF-A and Sema3A independently influence sympathetic neurite outgrowth and demonstrate higher Sema3A expression in non-innervated vessels, which coupled with the effect of exogenous Sema3A and VEGF-A on neurite growth suggests that Sema3A signaling exerts the predominant molecular influence and may promote sympathetic innervation of particular vessels in-vivo by reducing axon outgrowth towards sparsely innervated vessels.

Materials and methods

Mice

CD-1 mice were obtained from Charles River Laboratories (CRL Wilmington, MA) or laboratory stock derived from CRL breeders. VEGF-A (hi/+) mice, a generous gift from Dr. A. Nagy, (University of Toronto, Ontario, Canada) were generated as previously described (Miquerol et al., 1999; Nordal et al., 2004; Pinter et al., 2001) and bred in our animal facility. Specifically, VEGF-A–LacZ knock-in mice were generated by inserting an internal ribosome entry site (IRES)-LacZ cassette into the 3′ UTR (exon 8) of VEGF-A. This strategy permits the production of two functional proteins, VEGF-A and LacZ, from a single bicistronic transcript (Miquerol et al., 1999; Nordal et al., 2004; Pinter et al., 2001). In addition, addition of the LacZ cassette results in increased stability of VEGF-A mRNA, resulting in increased VEGF-A protein expression (Miquerol et al., 1999, 2000). Isolated vascular smooth muscle cells were isolated from mice expressing EYFP under the promoter for transgelin, a smooth muscle cell actin binding protein. Tg (Tagin-cre) 1HER mice on a mixed C57BL/6, SJL background (Jackson Laboratory, Bar Harbor, ME) were backcrossed to the conditional ROSA26-EYFP reporter strain (Srinivas et al., 2001).

Immunofluorescence

Femoral and carotid arteries were dissected from adult CD-1 mice, fixed in 4% paraformaldehyde in PBS (PFA), passed through a sucrose gradient as described (Li et al., 2007) and embedded in Tissue-Tek O.C. T Compound. 10 μm cryosections were incubated in blocking buffer (10% normal goat serum, 3% fetal bovine serum, 0.3% bovine serum albumin, 0.1% Triton-X in PBS) for 1 h before being transferred into primary antibody solution (rat anti-mouse PECAM-1, cat. # 550274, BD Biosciences, San Jose, CA; mouse anti-mouse smooth muscle alpha actin-Cy3 conjugated, cat. # C-6198, Sigma-Aldrich, St. Louis, MO; rabbit anti-mouse tyrosine hydroxylase, cat. # AB152, Chemicon, Temecula, CA; goat anti-rat vesicular acetylcholine transporter (VAChT), cat. # AB1578, Chemicon; and mouse anti-mouse synaptophysin, cat. # MAB5258, Chemicon) in blocking buffer overnight at 4 °C. Sections were washed and incubated in secondary antibody solution (Alexa Fluor 488 goat anti-rabbit, cat. # A11008; 594 goat anti-rabbit, cat. # A11012; 488 goat anti-rat, cat. # A11007; and 594 goat anti-mouse, cat. # A11005; Invitrogen, Carlsbad, CA) for 1 h. Coverslips were mounted with Vectashield containing DAPI (Vector Labs, Burlingame, CA).

VEGF-A (hi/+) innervation analysis

Femoral and carotid arteries were dissected from adult and postnatal day 16 mice, fixed, cryosectioned and stained for tyrosine hydroxylase immunoreactivity as described above. Total fluorescence intensity (integrated density) for tyrosine hydroxylase and the number of TH positive puncta were measured for each vessel using NIH ImageJ and divided by the vessel perimeter to calculate innervation density (intensity/μm) or # TH positive puncta (# TH positive puncta/μm).

Postnatal innervation analysis

Femoral and carotid arteries were dissected from mice between postnatal days 0–9, and were fixed in 4% PFA. Whole vessels were incubated in whole mount blocking buffer (4% normal goat serum, 0.1% Triton-X in PBS) for 1 h and then in primary antibody (rabbit anti-mouse tyrosine hydroxylase, cat. # MAB5258, Chemicon) overnight at 4 °C. Vessels were washed and incubated in the appropriate secondary antibody. To quench auto fluorescence, tissues were incubated in 0.05% Pontamine Sky Blue (Sigma-Aldrich) in PBS for 20 min. Vessels were then pinned at in situ dimensions on Sylgard® (#184; Dow Corning Corp., Midland, MI) on a glass slide. Innervation densities were determined by capturing image stacks with 2 μm steps through the *Z*-axis of the vessel using a Zeiss Axiovert 200 (10× objective) coupled to Axiovision software. Images were transferred into the NeuroLucida system (MicroBrightField, Williston, VT), which was used to trace the total nerve length on the superficial half of each vessel. Individual axons were joined artificially at nodes to produce a single nerve network with a spatial resolution of approximately 1 μm using NeuroExplorer (MicroBrightField, Williston, VT). Vessel surface area was determined by outlining each vessel to calculate the major and minor radii as well as the length of the vessel. Innervation density was then calculated as total nerve length (μm) / surface area of vessel (μm^2).

SCG explant co-culture

SCG were isolated from postnatal day 2 CD-1 mice. Non-neuronal cells were growth arrested with mitomycin C for 1 h (10 μg/ml, Sigma-Aldrich, St. Louis, MO). Carotid and femoral artery segments were harvested from adult CD-1 mice. Vessels were cleaned of adventitia and cut into 5 mm segments. Neurovascular co-cultures were embedded in type I collagen gel (150 μl, 2.5 mg/ml acid soluble bovine calf skin collagen (Madri et al., 1988)) in each well of a 24-well plate (as illustrated in Figs. 2A–C). Cultures were grown in a co-culture medium (DMEM/F12, 10% fetal bovine serum, 2 mM L-glutamine, 2 mM penicillin/streptomycin, and 20 ng/ml NGF) for 16 h (5% CO_2, 37 °C). For VEGF-A hypermorph co-cultures, femoral and carotid artery segments were isolated from VEGF-A (hi/+) mice. To block VEGF-A released from vessels, blocking antibodies directed towards human recombinant VEGF-A (R&D Systems) were used (1 μg/ml). Three independent experiments were performed that each included 4–5 SCG explants per culture condition (total $n = 14$). To block VEGF-A and/or Sema3A from vessel segments, a highly specific VEGFR2

inhibitor (VEGR2 Kinase Inhibitor I, Calbiochem, San Diego, CA; Sun et al., 1988), a function-blocking VEGFR1 neutralizing antibody (cat. # AF471, monoclonal anti-mouse VEGFR1, R&D Systems, Minneapolis, MN) or a function-blocking Nrp1 neutralizing antibody (cat. # AF566, anti-rat Nrp1, R&D Systems) was added to the media in indicated concentrations (total $n = 10–14$).

Imaging and morphological analysis

Ganglia were fixed in 4% PFA for 20 min at room temperature and visualized using an inverted light microscope (IX71-SIF; Olympus, Center Valley, PA) with CplanFL 4× NA 0.13 objective (Olympus) and captured with a digital camera (S97809; Olympus) using Picture Frame acquisition software (Optronics, Goleta, CA). Each SCG was divided into quadrants and images were obtained in the quadrants directed towards the femoral and carotid arteries (Fig. 2B). Average axon length (μm, 25 axons randomly selected per quadrant) was determined using NIH ImageJ. Ratios of directed neurite outgrowth were calculated to allow normalization across individual SCG explants. In outgrowth ratios represent outgrowth towards the innervated vessel (femoral) relative to that seen for the non-innervated vessel (carotid) except in instances where two carotid segments or two femoral segments are compared. In these instances, outgrowth towards the wild-type vessel is compared to the hypermorph (Fig. 4B).

Isolation of vascular smooth muscle cells

Whole femoral and carotid arteries were harvested from six-week old EYFP-transgelin mice. Vessels were washed two times in Hanks balanced salt solution (HBSS, Invitrogen) and incubated for 10 min at 37 °C in 1 mg/ml collagenase A (Sigma-Aldrich, St. Louis, MO) in HBSS. The adventitia was removed from all vessels, which were then pooled and washed twice in HBSS. Arteries were digested to single cell suspensions by incubating in 2 mg/ml collagenase A, and 0.5 mg/ml elastase (Sigma-Aldrich) for 30 min at 37 °C, triturating gently every 10 min. Following inactivation of the enzymes by adding 2 ml of media (DMEM, 10% fetal bovine serum, 1% penicillin/streptomycin), dissociated cells were collected by centrifugation at 1000 rpm for 10 min at room temperature and then plated in 2.5 ml media in a 35 ml tissue culture dish. Media was changed every three days and cells were split after approximately four weeks. Eight weeks post-isolation, cells were trypsinized and sorted by FACS to isolate only eYFP-positive femoral and carotid smooth muscle cells, which were then harvested to isolate total RNA as described below.

Quantitative real-time PCR

For analysis of mRNA expression of VEGF-A, Sema3A and their receptors in whole vessels, femoral and carotid arteries were dissected from postnatal day 2 mice and enzymatically digested (100 mg/ml hyaluronidase, 200 mg/ml type II collagenase, and 10 μg/ml proteinase K in DMEM) for 30 min at 37 °C. To obtain enough total RNA for analysis, vessels from 8–10 animals were pooled. For analysis of mRNA expression in isolated vascular smooth muscle cells, cells isolated from 12 animals were pooled and collected immediately after FACS sorting, as described above. RNA was extracted using Trizol reagent (Invitrogen, Carlsbad, CA) and its integrity was assessed by an Agilent Bioanalyzer (W.M. Keck Facility, Yale University) before being reverse transcribed (iScript, Bio-Rad Laboratories, Inc., Hercules, CA). Real time-PCR was carried out on an iCycler (Bio-Rad) using iQ SYBR-Green Master mix in the presence of exon-spanning oligonucleotide primers for VEGF-A and Sema3A (designed using PrimerQuest, Integrated DNA Technologies, Coralville, IA, Fig. 3A) (Wang and Seed, 2003). β-actin was used as an internal control to normalize samples. The amplification efficiencies of target (VEGF-A and Sema3A) and reference (β-actin) genes were analyzed and found to be equal. Melt curve analysis and ethidium bromide agarose gel electrophoresis were performed to evaluate PCR products. Relative quantification of fold-change in mRNA expression was calculated using the 2-DDCT method (Livak and Schmittgen, 2001). To calculate femoral vs. carotid expression, carotid arteries were used as control samples, and to calculate carotid vs. femoral expression femoral arteries were used as controls.

PCR

Reverse Transcription-PCR was performed on femoral and carotid cDNA using Clontech Advantage 2 PCR mix in the presence of exon-spanning oligonucleotide primers for VEGFR2, Nrp1 and Plexin A1 (designed using PrimerQuest, Integrated DNA Technologies or from Harvard Primer Bank [noted by Primer Bank ID numbers, Spandidos et al., 2008; Wang and Seed, 2003]) (Fig. 3A) using a PTC-200 Thermal Cycler (MJ Research, Waltham, MA). Following amplification, PCR products were analyzed using ethidium bromide agarose gel electrophoresis.

Western blot

Femoral and carotid arteries were dissected from postnatal day 2 CD-1 mice, washed in PBS to remove blood, and homogenized in lysis buffer (50 mM Tris, pH 8.0, 150 mM NaCl, and 1% NP-40). Vessels were pooled as described above. A bicinchoninic acid (BCA) assay (Thermo Scientific, Rockford, IL) was used to measure protein concentration and electrophoresis and membrane transfer was performed using constant protein load as described previously (Li et al., 2007). Membranes were blocked for 1 h (Tris-buffered saline/0.05% Tween 20 (TBST)/5% nonfat dry milk) and incubated overnight at 4 °C in primary antibody solution (goat anti-mouse Sema3A, cat. # sc-1148; rabbit anti-mouse VEGF-A, cat. # sc-507; Santa Cruz Biotechnology, Santa Cruz, CA). β-actin (mouse anti-mouse, cat. # A5316 Sigma-Aldrich, St. Louis, MO) was used as a normalizing protein. Membranes were washed and incubated in the appropriate secondary antibody (HRP-conjugated secondary antibodies, cat. # sc-2313 and sc-2314, Santa Cruz Biotechnology) for 1 h at room temperature. Horseradish peroxidase was detected with enhanced chemiluminescence (Pierce, Rockland, IL) and captured on autoradiographic film. Relative intensities of bands representing proteins of interest were quantified using Quantity One software (Bio-Rad Laboratories).

Immunostaining on isolated sympathetic neurons and whole SCG explants

SCG were dissected from postnatal day 2 CD-1 mice and cleaned of excess connective tissue, washed twice in sterile Hanks Balanced Salt Solution (HBSS, Invitrogen) to remove any remaining media and incubated in 0.025% trypsin for 30 min at 37 °C. SCG were washed twice in media (DMEM/F12, 10% fetal bovine serum, 2 mM L-glutamine, 2 mM penicillin/streptomycin, and 20 ng/ml NGF) to inactivate the trypsin and then triturated gently with a glass Pasteur pipette to dissociate the neurons. Dissociated cells were centrifuged (200 *g*, 5 min) in a swinging bucket rotor (Sorvall, GLC-2B), resuspended in fresh media and preplated on uncoated plastic tissue culture plates for 1 h (5% CO_2, 37 °C) before plating on pre-coated (100 μg/ml poly-L-lysine, 10 μg/ml laminin) 8-well chamber slides (cat. # 354108, BD Biosciences), and cultured for 16 h. Neurons were fixed in 4% PFA for 20 min at room temperature followed by blocking and permeabilization in blocking buffer (4% normal goat serum, 0.1% Triton-X in PBS) for 1 h at room temperature. Cells were then incubated overnight at 4 °C in the appropriate primary antibody diluted in blocking buffer (1:100 polyclonal rabbit anti-human VEGFR2, cat. # 2479, Cell Signaling Technology, Danvers, MA;

polyclonal rabbit anti-human PlexinA1, cat. # ab23391, Abcam, Cambridge, MA; polyclonal rabbit anti-human Flt1, cat. # sc-9029, and polyclonal rabbit anti-human neuropilin, cat. # sc-5541, Santa Cruz). Neurons were washed three times in PBS and then incubated in secondary antibody for 1 h at room temperature (1:100 Alexa Fluor 488 goat anti-rabbit, cat. # A11008, Invitrogen). Following another PBS wash, coverslips were mounted with Vectashield containing DAPI (Vector Labs, Burlingame, CA). Neurons were then visualized using an inverted microscope (IX71-SIF; Olympus, Center Valley, PA) with LCplanFL 20× NA 0.40 objective (Olympus) and captured with a digital camera (S97809; Olympus) using Picture Frame acquisition software (Optronics).

Whole P2 explants were dissected as described previously and cultured in the presence of femoral and carotid artery segments in 2.5 mg/ml collagen gel for 16 h. Ganglia were fixed in 4% PFA for 20 min at room temperature and washed three times in 1× PBS. Co-cultures were incubated in blocking buffer (4% normal goat serum, 0.1% Triton-X in PBS) for 2 h at room temperature and then in primary antibody (1:100 polyclonal rabbit anti-human VEGFR2, polyclonal rabbit anti-human PlexinA1, polyclonal rabbit anti-human Flt1, polyclonal rabbit anti-human neuropilin) diluted in blocking buffer overnight at 4 °C. Vessels were washed six times for 1 h at 4 °C in wash buffer (1% normal goat serum, 0.1% Triton-X in PBS) and incubated in goat anti-rabbit Alexa Fluor 488. Following six one-hour washes at 4 °C in wash buffer, co-cultures were imaged using a confocal microscope (Fluoview 200 Olympus, Center Valley, PA) with UPlanFl 10× NA 0.30 objective (Olympus).

SCG/VEGF-A and SCG/Sema3A sphere co-culture

Alginate spheres entrapping rhVEGF-A or rhSema3A/Fc were formed via an external gelation process. For all spheres, a 1% alginate (LVG, FMC Biopolymer, Philadelphia, PA) solution containing various concentrations of (0–10% w/v) rhVEGF-A_{165} or rhSema3A/Fc (Sema3A/Fc, R&D Systems, Minneapolis, MN) was added drop wise into an aqueous solution of 100 mM $SrCl_2$ through a 30-gauge needle to produce spheres approximately 1 mm in diameter. Spheres were allowed to cure for 10 min in solution, washed in dH_2O, snap frozen in liquid nitrogen and lyophilized. To determine the release profile (VEGF-A) or activity (Sema3A/Fc), spheres were embedded in 150 μl type I collagen gel in 1 ml co-culture medium and incubated at 37 °C. Media were removed at each time-point (1, 2, 4, 8, 12, 16 h) and replaced with fresh media. VEGF-A concentration in media samples was determined by ELISA (DuoSet, R&D Systems, Minneapolis, MN). Sema3A/Fc activity was assayed as described previously (Schwamborn et al., 2004). Briefly, 2×10^4 PC12 cells were seeded onto fibronectin coated coverslips in a 24-well plate and cultured for 24 h in PC12 media (DMEM, 10% heat-inactivated horse serum, 5% fetal bovine serum, 1% penicillin/streptomycin). Cells were then incubated in 16 h Sema3a/Fc conditioned media for 12 h, fixed with 4% PFA and stained with FITC-phalloidin to visualize neurites and growth cones. 50 ng/ml NGF was used as a positive control and blank sphere conditioned media served as a negative control. The percentage of cells extending neurites was counted and expressed as a percent of total cells.

For co-culture experiments, single alginate spheres were embedded in type I collagen gel 2 mm from postnatal day 2 SCG. Cultures were fixed after 16 h and co-cultures were analyzed as described above. For SCG/sphere co-cultures, measurements represent sphere/non-sphere directed neurite outgrowth. To block VEGF-A released from spheres, blocking antibodies directed towards human recombinant VEGF-A (clone JH121, cat. # 05-443, Millipore, Billerica, MA) or a highly specific VEGFR2 inhibitor (VEGR2 Kinase Inhibitor I, Calbiochem, San Diego, CA; Sun et al., 1988) were added to the media in indicated concentrations. Three independent experiments were performed with four or five SCG explants used per treatment in each (total $n=12$–14).

Vascular innervation co-cultures

Postnatal day 2 SCG were cultured in the presence of either adult femoral or carotid segments as described above for SCG explant co-cultures but were cultured for 5 days. Neurovascular co-cultures were immunostained as described above for whole SCG explants (rabbit anti-mouse tyrosine hydroxylase; goat anti-rabbit Alexa Fluor 488). Co-cultures were imaged using a confocal microscope (Fluoview 200 Olympus, Center Valley, PA) with UPlanFl 10× NA 0.30 objective (Olympus).

Statistics

The data were analyzed by ANOVA (StatView, SAS Institute Inc., Cary, NC) and reported as the mean ± standard error. Statistical significance was assumed when $p<0.05$.

Results

In rodents, post-synaptic sympathetic nerves densely innervate femoral, while the carotid artery can be considered sparsely innervated. To verify the vascular cell type innervated by sympathetic nerves, femoral and carotid artery segments were sectioned and stained with tyrosine hydroxylase (TH) to visualize axons, platelet endothelial cell adhesion molecule-1 (PECAM-1) to localize endothelial cells (EC) and smooth muscle alpha actin (SMAA) to visualize smooth muscle cells (SMC). In femoral segments, significant TH immunofluorescence was visible representing sympathetic innervation (Figs. 1A, B, D, E, G, H). Double-labeling with PECAM-1 and SMAA revealed that sympathetic varicosities are localized to the medio-adventitial border, closely approaching the SMC layer while failing to make contact with EC (TH/PECAM Figs. 1A–B, TH/SMAA Figs. 1D, E). Carotid arteries were devoid of TH fluorescence (Figs. 1C, F, I). To determine whether sympathetic nerves form synaptic contacts (varicosities) with vessels or simply travel along the vessel towards more distal targets, double-labeling was performed using TH and synaptophysin, a non-specific synaptic marker. Significant synaptophysin immunofluorescence was present at the medio-adventitial border of both the carotid and femoral arteries; however only in femoral artery segments were synapses co-labeled for TH and synaptophysin (Figs. 1G, H). While sympathetic innervation is absent from carotid artery sections (Figs. 1C, F, I), both carotid and femoral artery sections showed significant cholinergic innervation that co-localizes with synaptophysin (Figs. 1J, K).

To evaluate the changes in the density of femoral artery innervation during the early postnatal period, TH immunofluorescence and calculation of innervation density were performed on whole mount vessels between postnatal days 0 and 9 as well as adult vessels. Innervation densities were significantly different from adult (0.07 ± 0.006) between postnatal days 0 through 3 (0.037 ± 0.001 through 0.057 ± 0.002), after which there were no significant differences (Fig. 1L).

To determine whether differences in neurite outgrowth towards innervated (femoral arteries) and non-innervated (carotid arteries) vessels exist, a 3D co-culture system was used to quantify sympathetic axon length towards femoral and carotid artery segments. SCG explants from P2 mice and artery segments from adult mice were embedded in a type I collagen gel (Fig. 2A). Fig. 2B illustrates the TH positive baseline sympathetic neurite outgrowth from the SCG. When SCG were cultured alone, there was radial outgrowth around the entire SCG (data not shown). In single vessel co-cultures, when carotid artery segments alone were cultured with SCG explants, average neurite length decreased towards the vessel segment compared to that on the contralateral side ($20\pm5\%$, $n=14$, data not shown) and when femoral artery segments alone were co-cultured with SCG explants, there was an increased vessel directed neurite

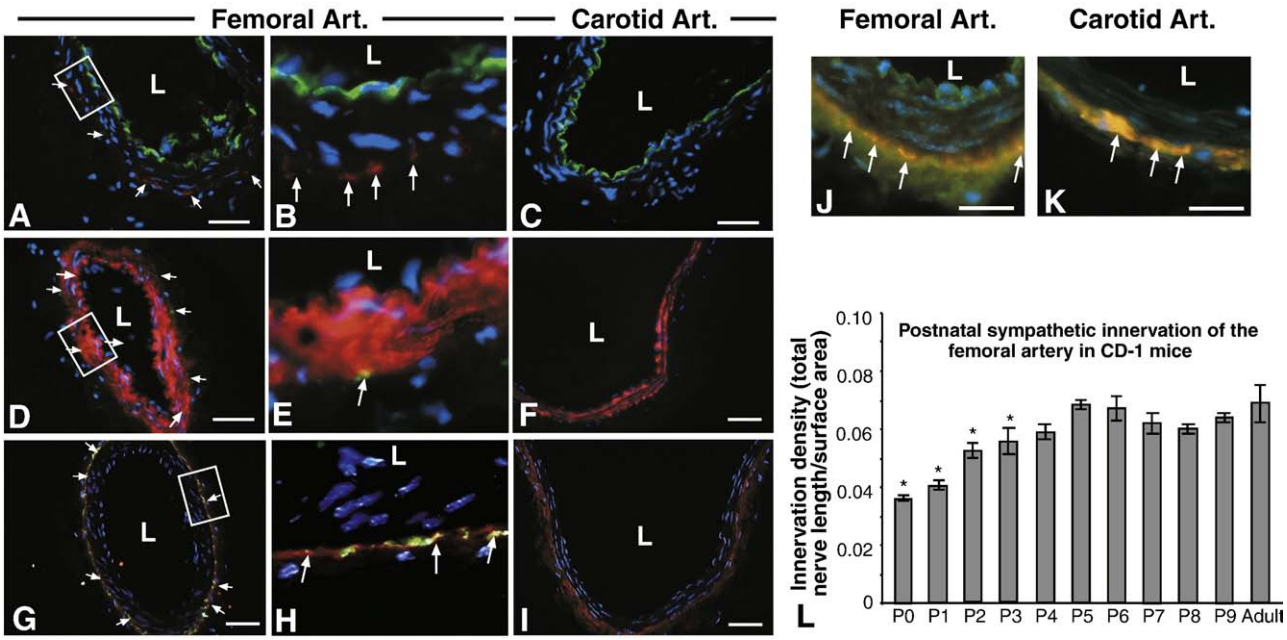

Fig. 1. Localization of murine vascular sympathetic innervation. (A–C) Immunolabeling for PECAM-1 (green) to mark vascular endothelial cells, tyrosine hydroxylase (red) to mark sympathetic nerves and DAPI (blue) to mark nuclei in femoral (A, B = boxed area in panel A) and carotid arteries (C). Localization of both tyrosine hydroxylase and PECAM-1 is found in adult femoral artery sections (A and B, arrows) but tyrosine hydroxylase localization is absent from adult carotid artery sections (C). L = lumen. Scale bar = 50 μm. (D–F) Immunolabeling for smooth muscle cell actin (red) to mark vascular SMCs, tyrosine hydroxylase (green) and DAPI (blue) to mark nuclei in femoral (D, E = boxed area in panel D) and carotid arteries (F). Innervation patterns match that of PECAM-1/TH double-labeling (D and E, arrows). Sympathetic nerves are localized to the medio-adventitial border of the femoral arteries (orange–yellow fluorescence — arrows). Scale bar = 50 μm. (G–I) Immunolabeling for synaptophysin (red) to mark synapses, tyrosine hydroxylase (green) to mark sympathetic nerves and DAPI (blue) to mark nuclei in femoral (G, H = boxed area in panel G) and carotid (I) artery sections. Both vessels show significant synapse formation around the periphery, but synapses with sympathetic nerves are localized only in femoral artery sections (G and H, orange–yellow fluorescence — arrows). Scale bar = 50 μm. (J and K) Immunolabeling for synaptophysin (red) to mark synapses, vesicular acetylcholine transferase (green) to mark sympathetic nerves and DAPI (blue) to mark nuclei in femoral (J) and carotid (K) artery sections. Both vessels show significant synapse formation around the periphery (orange–yellow fluorescence — arrows). Scale bar = 50 μm. (L) Innervation densities were quantified in femoral arteries from postnatal days 0 through 9 mice by whole mount tyrosine hydroxylase immunofluorescence. Innervation density was calculated as described in Materials and methods and represents total nerve length (μm) / surface area (μm^2) for the superficial half of each vessel. Significant differences between postnatal and adult innervation differences exist between days 0–3, after which no differences exist. Carotid arteries are not innervated (data not shown) ($n = 6$; vertical bars represent standard error; * = $p < 0.05$).

length (12% ± 3, $n = 14$, data not shown). When both vessels were used in a single co-culture, average neurite outgrowth towards the femoral artery was higher than carotid directed outgrowth (19 ± 5%) (Figs. 2C, D). Preliminary neurovascular co-cultures performed using P2 vessels and SCG showed similar results (15 ± 4%, $n = 8$, data not shown). Due to the fragility and size of P2 vessels, adult vessels were used in subsequent experiments because they are larger and easier to manage. In addition, following local freeze-damage, sympathetic reinnervation of adult begins within two weeks, suggesting that these vessels upregulate the expression of axon growth promoting guidance cues (Looft-Wilson et al., 2004). To evaluate whether the presence of the carotid or femoral artery is sufficient to disrupt the expected pattern of neurite outgrowth rearrangements of the vessels in the 3D co-culture were used (Fig. 2D). First we placed femoral arteries on the same side of the SCG as the carotid artery, either proximal (CFSF; C = carotid, F = femoral, S = SCG) or distal to the SCG (FCSF). No significant difference was observed in directed neurite outgrowth compared to that observed towards the carotid artery segment in the 3D co-culture (Fig. 2D). In contrast, the placement of carotid artery segments on the same side as the femoral artery either proximal (FCSC) or distal (CFSC) to the SCG blunted the femoral artery mediated neurite outgrowth (Fig. 2D).

As both VEGF-A and Sema3A have been implicated in neuronal survival, proliferation and axon outgrowth via interactions with neuropilin-1 and VEGFRs, we tested their ability to influence SCG outgrowth. First, we evaluated the expression of both growth factors and their receptors by quantitative real-time PCR (qRT-PCR) to measure mRNA levels and Western blot to determine protein expression in both whole vessel and isolated smooth muscle cells (SMC). In both whole femoral arteries, VEGF-A mRNA expression was three-fold higher compared to the carotid artery. In contrast, Sema3A mRNA showed an opposite trend of the same magnitude (Fig. 3B). In isolated SMC, VEGF-A mRNA expression was approximately 1.5-fold higher in femoral SMC compared to carotid SMC, while Sema3A mRNA was three-fold higher in carotid compared to femoral SMC (Fig. 3B). Analysis of mRNA levels revealed that Nrp-1, Plexin A1 and VEGFR2 are present in SCG explants as well as in vessels (Fig. 3C). To evaluate whether the presence of vessels elicited a change in localization of these receptors SCG, whole explants were co-cultured alone or with femoral and carotid artery segments and immunofluorescent staining was performed for Nrp-1, PlexinA1, VEGFR2 and VEGFR1. There were no changes in localization of these receptors between SCG cultured alone and SCG co-cultured with innervated and non-innervated vessel segments (Supplementary Figure 4). To ensure that the expression of these receptors was specific to sympathetic neurons and not the result of capillaries in the SCG, immunofluorescent staining was performed on dissociated SCG neurons (Fig. 3D). All four receptors were expressed in dissociated sympathetic neurons. VEGFR2, PlexinA1 and Nrp-1 appeared to be localized throughout the neuron while VEGFR1 appeared to be restricted primarily to the cell body, although faint immunofluorescence was observed along the axon (Fig. 3D). Despite the significant difference in VEGF-A mRNA expression in femoral vs. carotid, there were no significant differences in VEGF-A protein expression in whole vessels. However, Sema3A expression was significantly higher in the carotid artery compared to the femoral artery whole vessel lysates (Figs. 3E, F).

Next we explored the role of vascular-derived VEGF-A in promoting sympathetic neurite outgrowth. VEGF-A (hi/+) mice exhibit subtle but significant increases in femoral artery sympathetic innervation density compared to wild-type littermates both as adults

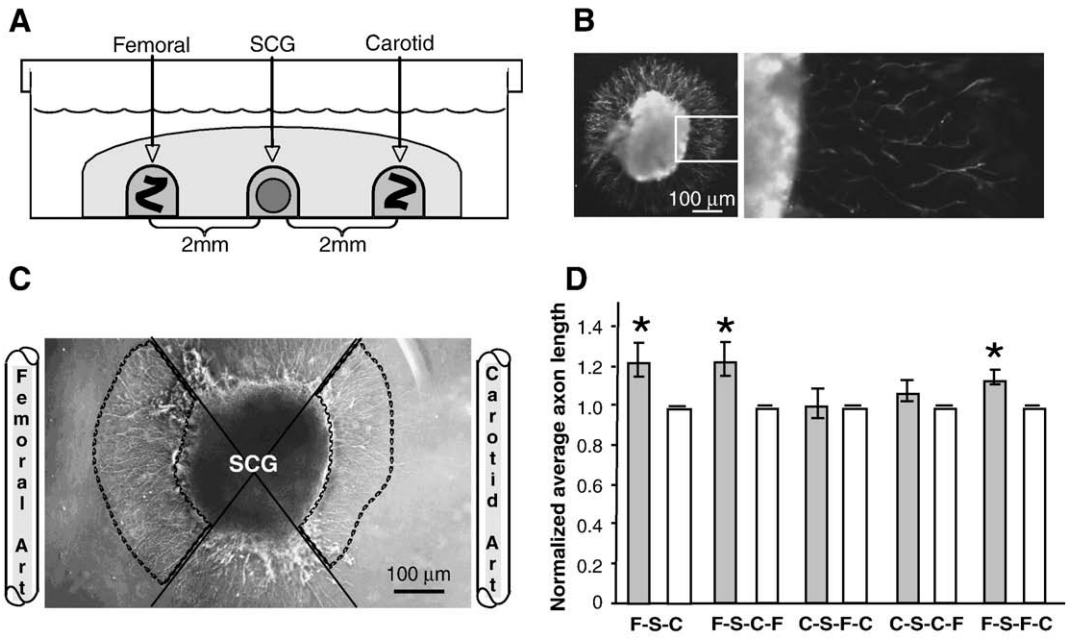

Fig. 2. Directed migration in neurovascular co-cultures. (A) Schematic representing three-dimensional in-vitro co-culture. Whole SCG explants from postnatal day 2 mice were co-cultured in the presence of adult femoral and carotid artery segments. Tissues were embedded in type I collagen gel 2 mm apart and cultured for 16 h. (B) Tyrosine hydroxylase immunolabeling in whole SCG explants. Left, low magnification; right (boxed inset), high magnification. Scale bar = 100 μm. (C) Representative image of SCG co-cultured with femoral and carotid artery segments. Femoral and carotid artery segments were placed 2 mm from SCG explants. To quantify outgrowth, the area occupied by the SCG and its neurites was divided into quadrants (solid lines). Average axon length was measured for 25 axons in the femoral and carotid directed quadrants (outlined by dashed lines). Carotid directed average axon length was normalized to 1 and femoral/carotid ratios were calculated. Scale bar = 100 μm. (D) Directed neurite outgrowth of sympathetic axons from whole SCG explants. Neurites of equal average length grew radially from SCG alone controls (data not shown). In femoral/carotid co-cultures (first pair of bars) (FSC) the average axon length was significantly increased towards the femoral compared to the carotid artery. ($n = 14$; $* = p < 0.05$; vertical bars represent standard error.) To test the effect of vessel rearrangements on directed neurite outgrowth, SCG explants (S) were cultured in the presence of various arrangements of vessels. When femoral segments (F) were placed on the same side as carotid segments (C), either proximal (second pair of bars) (FSCF) or distal to the SCG (S) (third pair of bars) (CSFC) outgrowth towards the femoral segment was blunted, with the placement of carotid segments disrupting the typical increased outgrowth observed towards femoral segments. ($n = 14$; $* = p < 0.05$; vertical bars represent standard error.) When femoral segments (F) were placed on the same side as carotid segments (C), either distal (fourth pair of bars) (CSCF) or proximal to the SCG (S) (fifth pair of bars) (FSFC) outgrowth towards the carotid segment was unchanged.

and at postnatal day 16 as measured by calculating both integrated density/μm (Fig. 4A) and by counting the number of tyrosine hydroxylase positive puncta (Fig. 4B). In both wild-type and VEGF-A (hi/+) littermates, the common carotid is not innervated by sympathetic nerves. Co-culture experiments using wild-type SCG and vessel segments from wild-type mice and mice exhibiting high (VEGF-A (hi/+) VEGF-A expression (Miquerol et al., 1999, Miquerol et al., 2000) were used to further evaluate the role of VEGF-A in modulating vascular sympathetic outgrowth (Fig. 4C). Both femoral and carotid arteries express approximately 40% higher levels of VEGF-A mRNA and protein compared to wild-type littermates (Supplementary Figure 1). Because femoral arteries express little Sema3A (Figs. 3E–F), Sema3A expression levels in VEGF-A (hi/+) carotid vessels were evaluated and were found to be no different from wild-type littermates (Supplementary Figure 1). Vessels harvested from wild-type littermates displayed no deviation from the expected patterns of outgrowth with increased average axon length towards the femoral compared to the carotid artery ($18 \pm 4\%$, $n = 12$) (Fig. 4C, second pair of bars, WF-S-WC). This also occurred when VEGF-A (hi/+) femoral artery segments were used ($20 \pm 5\%$, $n = 12$) (Fig. 4C, third pair of bars, VF-S-WC). However, when VEGF-A (hi/+) carotid artery segments were used in co-culture with wild-type femoral segments, the pattern of outgrowth was reversed. Average axon length was increased towards the VEGF-A (hi/+) carotid artery compared to the femoral artery ($13 \pm 4\%$, $n = 12$) (Fig. 4C, fourth pair of bars, WF-S-VC). When both femoral and carotid segments were from VEGF-A (hi/+) mice, there was no significant difference in outgrowth towards either vessel (Fig. 4C, first pair of bars, VF-S-VC). Co-cultures were performed with either carotid or femoral arteries from wild-type and VEGF-A (hi/+) littermates. In both carotid–carotid and femoral–femoral vessel co-cultures, outgrowth towards the VEGF-A (hi/+) was significantly higher than towards the wild-type vessel (Fig. 4C, fifth and sixth pairs of bars, WC-S-VC, WF-S-VF). The effect of increased VEGF-A was more significant in carotid vs. femoral cultures ($15 \pm 4\%$, $8 \pm 2\%$) suggesting that VEGF-A may provoke a larger outgrowth response in carotid arteries. To block VEGF-A released from vessels, VEGF-A blocking antibodies were included in VEGF-A (hi/+) co-cultures. In WF-S-WC, VF-S-WC and WF-S-VC co-cultures, inclusion of the blocking antibody was able to blunt the increase in outgrowth observed towards one vessel compared to the other (Supplementary Figure 2). In VF-S-VC co-cultures, the antibody restored the increased outgrowth observed towards the femoral artery observed in wild-type neurovascular co-cultures.

Additionally, we evaluated the effect of increased exogenous rhVEGF-A on SCG explants. Single alginate spheres loaded with known amounts (w/v) of human recombinant VEGF-A were used in co-culture with SCG explants to evaluate directed axon outgrowth towards known VEGF-A gradients. Mouse and human VEGF-A share approximately 90% homology and human VEGF-A has been used in previous studies using mouse cells (Smith et al., 2004). Quantitative VEGF-A release profiles of VEGF-A/alginate spheres containing various w/v percentages of VEGF-A (0.6%, 1.25%, 2.5%, 5% and 10%) were observed to exhibit reproducible, quantifiable release profiles into media over the 16 h time frame of the co-culture experiments (0 ng/ml, 1.2 ± 0.2 ng/ml, 16.9 ± 2.8 ng/ml, 26.0 ± 4.4 ng/ml, and 67.0 ± 14.0 ng/ml respectively; Fig. 4C). Release profiles were also performed for VEGF-A spheres embedded in 2.5 mg/ml collagen gel, which produced similar trends for release, although the magnitude of release into the media was decreased compared to media alone. This is likely caused by association of VEGF-A molecules with the

A

PRIMER (MOUSE)	PRIMER BANK ID	SEQUENCE
VEGF forward	6678563a1	GCACATAGGAGAGATGAGCTTCC
VEGF reverse		CTCCGCTCTGAAGCAAGGCT
Sema3A forward	31543681a1	GAAGAGCCCTTATGATCCCAAAC
Sema3A reverse		AGATAGCGAAGTCCCGTCCC
VEGFR2 forward	27777648a1	TTTGGCAAATACAACCCTTCAGA
VEGFR2 reverse		GCAGAAGATACTGTCACCACC
Neuropilin1 forward	6679134a3	CGTGGAAGTAATTGATGGGGAG
Neuropilin1 reverse		GGACTTTATACTCCAGTAGGTGC
Plexin A1 forward	Designed using PrimerQuest (IDT DNA, Coralville, IA)	GGGTGTGTGGATAGCCATCAG
Plexin A1 reverse		GCCAACATATACCTCTCCTGTCT
βactin forward	Designed using PrimerQuest (IDT DNA, Coralville, IA)	GTGATGGTGGGAATGGGTCAGAAT
βactin reverse		TGTGGTGCCAGATCTTCTCCATGT

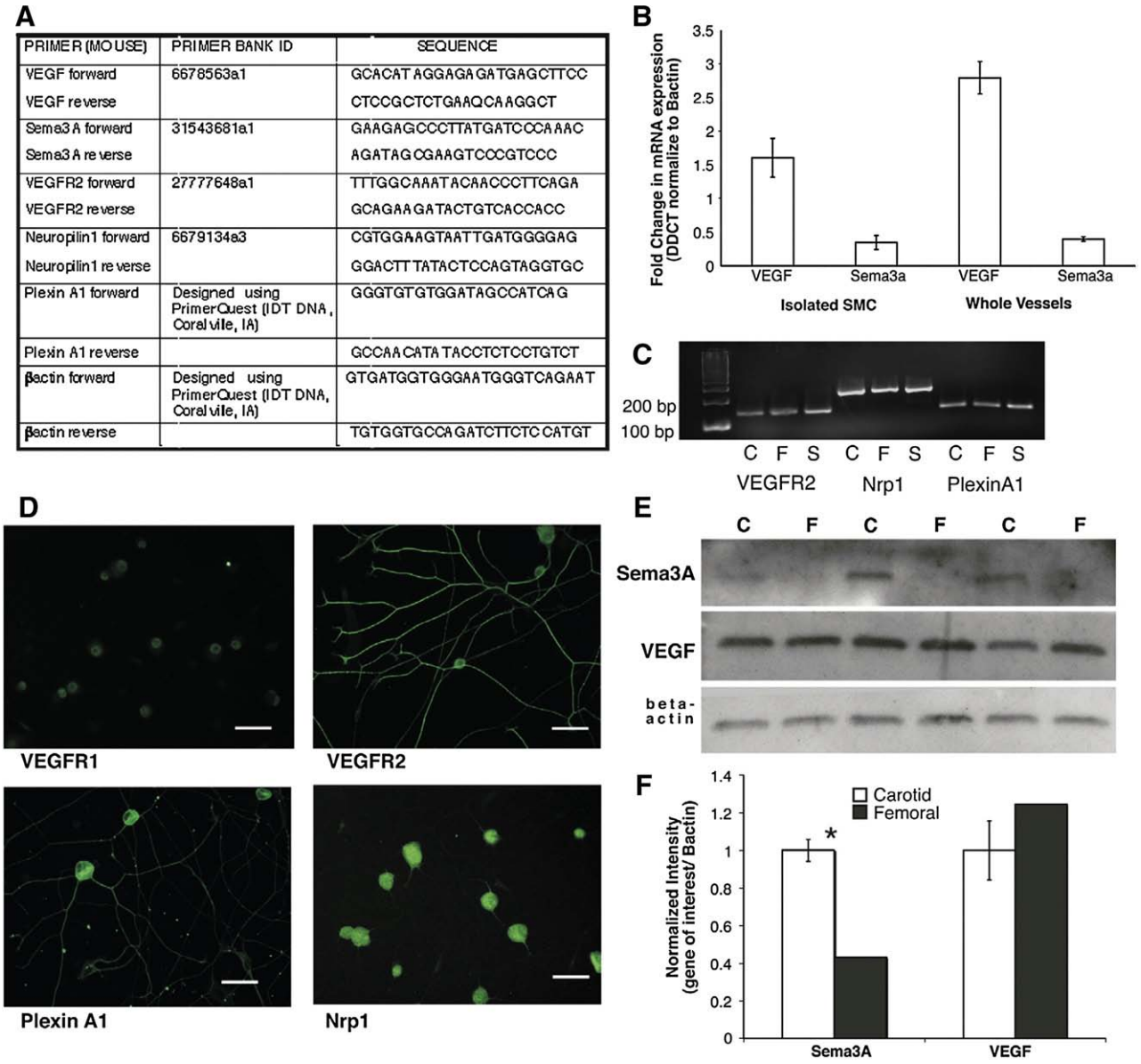

Fig. 3. Expression of guidance cues and their receptors in vessels and SCG. (A) VEGF-A, Sema3A, VEGFR2, Nrp1 and PlexinA1 forward and reverse primer sets used for quantitative real-time PCR and RT-PCR. (B) Quantitative real-time PCR analysis of VEGF-A and Sema3A in femoral and carotid artery isolated smooth muscle cells (SMC) and whole vessels. Femoral arteries and SMC express a three-fold increase in VEGF-A mRNA compared to carotid arteries and SMC while the expression profile of Sema3A in the reciprocal. ($n=3$ for each gene of interest; $*=p<0.05$; vertical bars represent standard error.) (C) RT-PCR analysis of receptor expression in vessels and SCG. Femoral and carotid arteries as well as SCG express mRNA for VEGFR2, Nrp1 and PlexinA1. (D) Immunofluorescent analysis of VEGFR1, VEGFR2, PlexinA1 and Nrp1 in postnatal day 2 dissociated SCG neurons. Scale bar = 50 μm. (E) Protein expression of guidance cues in postnatal day 2 whole vessel lysates. Representative Western blots of femoral (F) and carotid (C) artery segments identifying Sema3A and VEGF-A normalized to beta actin. (F) Quantification of Western blot data. Sema3A expression is significantly higher in carotid compared to femoral artery segments while VEGF-A expression is not significantly different between vessels ($n=3$ for each gene of interest; $*=p<0.05$; vertical bars represent standard error).

collagen gel, which would reduce VEGF-A diffusion into the media. In co-culture with SCG explants, there was no significant difference in average axon length towards empty spheres or towards 0.6% w/v VEGF-A spheres (Fig. 4E.) Increases in outgrowth towards VEGF-A containing spheres were dose-dependent with the highest increase in outgrowth towards spheres containing 2.5% w/v VEGF-A ($25\pm7\%$ higher than towards empty spheres, Fig. 4E). In addition, there were no significant differences in axon length towards the 5% and 10% spheres compared to that towards blank spheres (Fig. 4E). To determine whether these effects were due specifically to VEGF-A, human VEGF-A neutralizing antibodies were used to sequester exogenous VEGF-A that diffused from the alginate spheres into the collagen gel in SCG alone cultures. Concentrations as low as 500 ng/ml of neutralizing antibody were able to block the outgrowth-promoting effect of 2.5% VEGF-A spheres in SCG co-cultures (Fig. 5A, axon length normalized to no-antibody control). When lower concentrations of VEGF-A neutralizing antibody were used (100 and 250 ng/ml) there was no effect of the antibody on expected neurite outgrowth compared to 2.5% VEGF-A sphere controls without antibody. In addition, a highly selective cell permeable VEGFR2 tyrosine kinase inhibitor (Sun et al., 1988) was able to similarly block the increased average axon length towards 2.5% VEGF-A spheres at concentrations as low as 1 μM (Fig. 5B, axon length normalized to no inhibitor control). To evaluate whether the growth promoting effect of femoral arteries may be attributed to VEGF-A signaling SCG–femoral co-cultures were performed using various concentrations of VEGFR2 inhibitor (Fig. 5C, vessel and non-vessel average axon length at all concentrations of inhibitor was

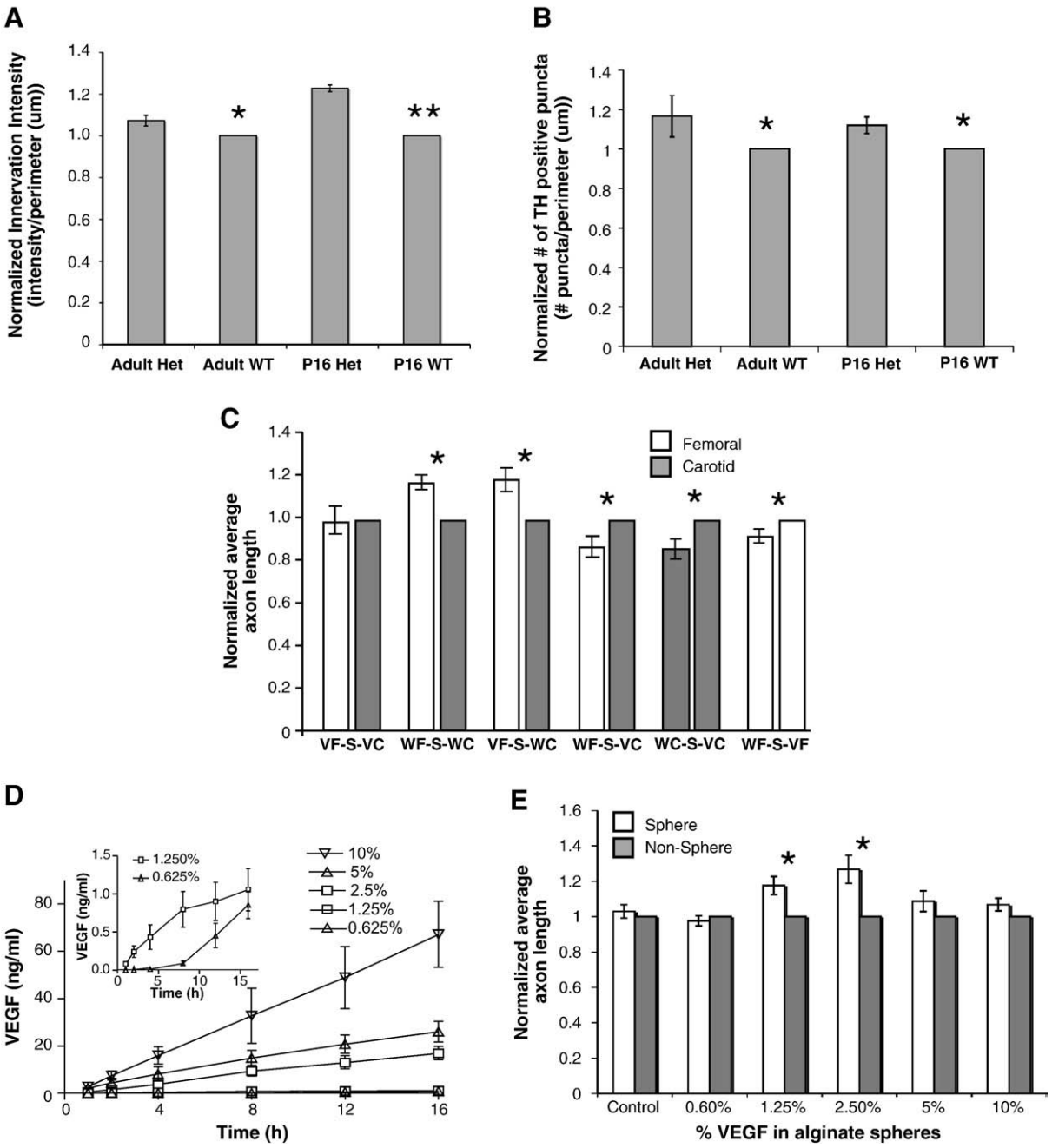

Fig. 4. The effect of VEGF-A on directed neurite outgrowth (unless otherwise noted $n=14$, vertical bars represent standard error). (A, B) Innervation analysis of sympathetic innervation in VEGF-A (hi/+) compared to wild-type littermates. Tyrosine hydroxylase immunostaining revealed significant increases in sympathetic innervation density measured by both immunofluorescence intensity (A) and # of TH positive puncta (B) in both adult and postnatal day 16 compared to matched WT controls. ($n=5$ for each age group; $*=p<0.05$, $**=p<0.01$.) (C) Neurovascular co-cultures using vessels from VEGF-A (hi/+) heterozygous mice and wild-type littermates. When placed on either side of SCG, VEGF-A (hi/+) carotid and femoral artery segments elicited an increased equal neurite outgrowth compared to wild-type carotid segments, reflecting increased VEGF-A expression in both vessel segments (first pair of bars), in contrast to the differential neurite outgrowth towards femoral artery segments observed when wild-type vessel segments were used (second pair of bars). Similar outgrowth was noted when VEGF-A (hi/+) femoral artery segments (VF) were compared to wild-type carotid artery segments (WC) (third pair of bars). VEGF-A (hi/+) carotid artery segments (VC) promoted increased average axon length from the SCG (S) when cultured with both wild-type femoral (WF) (fourth pair of bars) and wild-type carotid (WC) (fifth pair of bars) vessel segments. Lastly, VEGF-A (hi/+) (VF) femoral segments elicited increased outgrowth compared to wild-type femoral artery segments (WF) (sixth pair of bars). Interestingly, femoral artery segments from VEGF-A (hi/+) (VF) mice did not promote further increases in expected average axon length when cultured with wild-type carotid artery segments (WC) than did wild-type femoral artery segments (WF) (compare the second and third pairs of bars). ($*=p<0.05$.) (D) Release of VEGF-A into type I collagen gel from VEGF-A/alginate spheres by ELISA. VEGF-A/alginate spheres released increasing amounts of VEGF-A into the media over 16 h. Amounts of VEGF-A released ranged from 70 ng/ml (10% w/v VEGF-A) to 1.5 ng/ml (1.25% and 0.625% w/v VEGF-A, inset). (E) SCG outgrowth in response to VEGF-A/alginate spheres. Average sympathetic neurite lengths towards 2.5% and 1.25% w/v VEGF-A/alginate spheres was approximately 25% and 18% higher respectively compared to the non-vessel quadrant. Control, 0.625%, 5% and 10% w/v spheres caused no significant increases in outgrowth. ($*=p<0.05$.)

normalized to no inhibitor control). Similar to SCG–VEGF-A sphere co-cultures, the VEGFR2 inhibitor was able to decrease overall neurite outgrowth towards both the vessel and non-vessel directions in a dose-dependent manner using concentrations as low as 1 μM. However, when average outgrowth towards the non-vessel direction was normalized to vessel-directed (femoral) outgrowth, at all concentrations of VEGFR2 inhibitor there was still an increased outgrowth towards the artery (Fig. 5D, non-vessel-directed axon

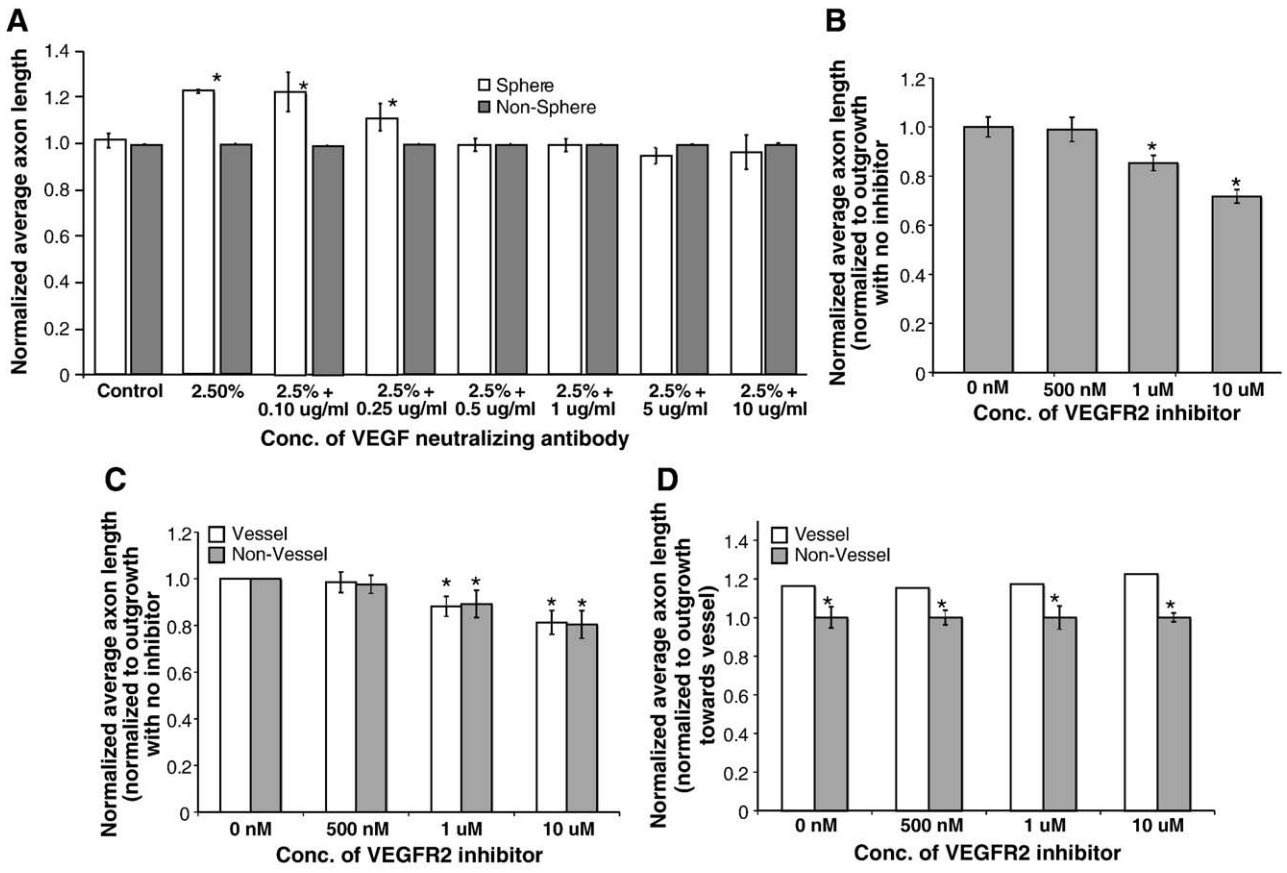

Fig. 5. The effect of VEGF-A neutralization on directed neurite outgrowth ($n=14$, vertical bars represent standard error). (A) The effect of VEGF-A neutralizing antibodies on average axon length. Anti-human VEGF-A antibodies were used to neutralize the effect of VEGF-A released from alginate spheres. Concentrations as low as 500 μg/ml were able to block the effect of the VEGF-A/alginate spheres compared to sphere alone controls. ($*=p<0.05$.) (B) The effect of a VEGFR2 inhibitor on average axon length. A highly specific cell permeable VEGFR2 tyrosine kinase inhibitor was used to block signaling from VEGF-A released from alginate spheres. Concentrations as low as 1 μg/ml were able to block the effect of VEGF-A/alginate spheres compared to sphere alone controls (first bar on the left). (C) The effect of the VEGFR2 inhibitor on femoral–SCG neurovascular co-cultures. The cell permeable VEGFR2 inhibitor was also able to decrease neurite outgrowth elicited by femoral artery segments co-cultured with SCG. ($*=p<0.05$.) Average axon length (for vessel and non-vessel cultures) at all inhibitor concentrations is normalized to axon lengths with no VEGFR2 inhibitors. On both the vessel and non-vessel sides of the SCG, there is a decreased average axon length compared to the no inhibitor control (first pair of bars on the left). (D) The effect of VEGFR2 inhibitors on the increase in axon outgrowth elicited by femoral artery segments. At each concentration of VEGFR2 inhibitor, average axon length on the non-vessel side of the SCG is normalized to the average axon length towards the vessel. Although VEGFR2 tyrosine kinase inhibitors were able to significantly decrease overall axon length in femoral–SCG neurovascular co-cultures at all inhibitor concentrations tested, the ratio of vessel/non-vessel outgrowth was maintained with significantly more outgrowth observed in the quadrant towards the femoral artery segment compared to the non-vessel quadrant. ($*=p<0.05$.)

length normalized to vessel directed axon length at each inhibitor concentration).

To evaluate the effect of other VEGF-A receptors in directed neurite outgrowth, VEGFR1 and Nrp1 function-blocking antibodies were used in SCG alone and neurovascular co-cultures. VEGFR1 antibodies had no effect SCG cultures (Supplementary Figure 3A) or on the overall average axon length in femoral–SCG co-cultures at all concentrations tested (Supplementary Figure 3B; vessel and non-vessel average axon length at all concentrations of inhibitor was normalized to no inhibitor control). In addition, when average outgrowth towards the non-vessel direction was normalized to vessel-directed (femoral) outgrowth, VEGFR1 antibodies were also unable to alter the expected pattern of outgrowth and there was an increased average axon length towards the vessel (Fig. 3C; non-vessel-directed axon length normalized to vessel directed axon length at each inhibitor concentration).

Similar co-culture experiments to those conducted with VEGF-A were performed to evaluate the effects of Sema3A in promoting or repressing sympathetic neurite outgrowth. Alginate spheres encapsulating known amounts (0%, 1.25%, 2.5% and 5% w/v) of recombinant chimeric human Sema3A/Fc were used in co-culture with SCG explants to evaluate directed axon outgrowth towards gradients of Sema3A. As with VEGF-A, mouse and human Sema3A share a high degree of homology and Sema3A/Fc has been used in-vitro with mouse neural crest cells (Xu et al., 2006). Due to the lack of reagents of required sensitivity, it was not possible to determine the exact release profile of Sema3A from alginate spheres. However, we conducted neurite outgrowth assays using PC12 cells in the presence of Sema3A/alginate sphere conditioned media. Our results suggested that as Sema3A increased, the percentage of PC12 cells that produced neurites increased (data not shown). In co-culture with SCG explants, average axon length towards Sema3A containing alginate spheres decreased in a dose-dependent manner compared to axon length towards empty spheres. Average axon length towards the 1.25% w/v and 2.5% w/v Sema3A/Fc spheres was decreased by approximately $14\pm3\%$ and $16\pm3\%$ respectively compared to outgrowth towards blank spheres in the same well (Fig. 6A). As with the VEGF-A encapsulated spheres, there were no significant differences in axon length towards the 5% w/v spheres compared to that towards the blank spheres (Fig. 6A). Due to the limited availability of specific Sema3A inhibitors/antagonists that do not act by blocking Nrp1 signaling, it was not possible to evaluate their effects on neurite outgrowth.

To evaluate if either growth factor signaling pathway predominates in our in-vitro co-culture, SCG cultures were performed in the presence of both VEGF-A and Sema3A/Fc-encapsulated alginate spheres, either on opposing sides of the SCG or in combination on the same side. First, experiments were conducted with alginate spheres on opposing sides of the SCG. When 2.5% w/v VEGF and

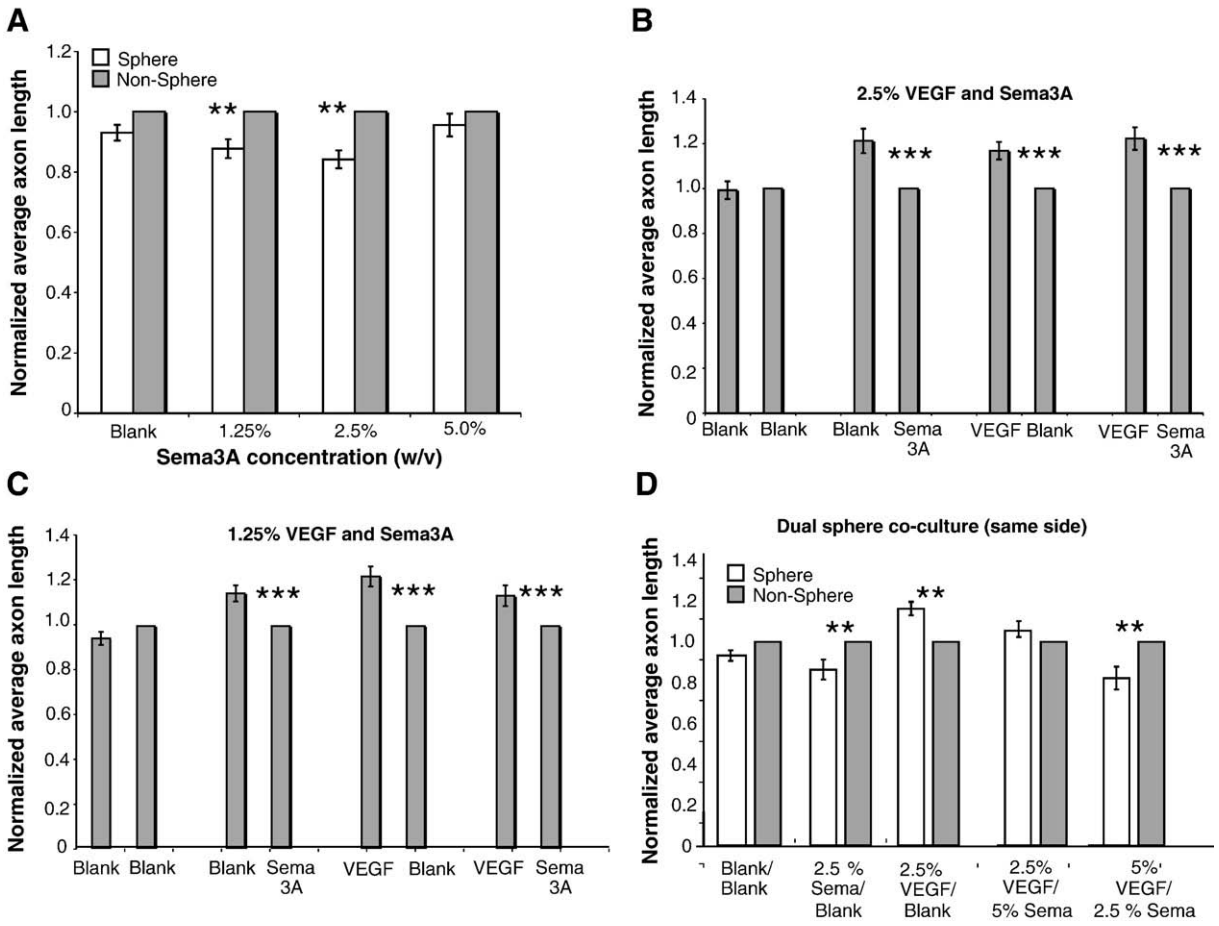

Fig. 6. The effect of Sema3A on directed neurite outgrowth ($n = 14$, vertical bars represent standard error). (A) SCG outgrowth in response to Sema3A/alginate spheres. An average sympathetic neurite length towards 1.25% and 2.5% Sema3A/alginate spheres was decreased by approximately 25% compared to empty spheres. 5% Sema3A/alginate spheres caused no significant decrease in neurite outgrowth. (** = $p<0.01$.) (B, C) SCG outgrowth in response to VEGF-A/alginate and Sema3A/alginate spheres placed on opposite sites of the SCG. Average neurite outgrowth towards VEGF-A spheres was 17% higher compared to empty spheres and was decreased by 21% towards Sema3A spheres compared to empty spheres. There were no significant differences when VEGF-A and Sema3A spheres were used in combination in dual sphere cultures compared to single sphere cultures at either 2.5% (B) or 1.25% (C) VEGF and Sema3A. (** = $p<0.001$.) (D) SCG outgrowth in response to VEGF-A/Sema3A/Blank alginate spheres. Alginate spheres were placed in combination on the same side of the SCG. Neurite outgrowth towards VEGF-A/Blank spheres was 16.5% higher and towards the Sem3A/Blank spheres was 14% lower compared to the non-sphere side. When 2.5% VEGF-A and a 5% Sema3A spheres were used, there was only a 6% increase in outgrowth towards the spheres compared to the non-sphere side. When 5% VEGF-A and 2.5% Sema3A spheres were used, there was an 18% decrease in outgrowth compared to the non-sphere side. (* = $p<0.05$.)

Sema3A alginate spheres were used in co-culture with SCG, outgrowth patterns were similar to those seen in single sphere co-cultures with approximately $22 \pm 5\%$ increased growth towards the VEGF-A containing sphere compared to the Sema3A sphere (Fig. 6B). Similar patterns of outgrowth were seen when 1.25% w/v spheres were used, although the magnitude of the difference was decreased ($13 \pm 4\%$ increased outgrowth towards the VEGF-A sphere) which is similar to the decrease in outgrowth observed when 1.25% w/v spheres were used in single sphere co-cultures (Fig. 6C). Since co-culture experiments utilizing equal concentrations of spheres produced similar results to individual sphere experiments, co-cultures were performed that included varied concentrations of VEGF-A and Sema3A/Fc spheres. We evaluated the effect of VEGF-A and Sema3A spheres on neurite outgrowth when the spheres were both placed on the same side of the SCG, creating a combinatorial effect of their concentration gradients. Again, we used VEGF-A/Blank and Sema3A/Blank cultures as controls and results were not significantly different from our original alginate sphere studies (Figs. 4D, 6A–C). When 2.5% w/v Sema3A and blank spheres were used on the same side of the SCG, there was a decrease in outgrowth own the sphere side of the SCG of approximately $14 \pm 5\%$ (Fig. 6D, second pair of bars). When 2.5% VEGF-A and blank spheres were placed on the same side of the SCG, there was an approximately $16 \pm 3\%$, increase in growth towards the spheres (Fig. 6D, third pair of bars). Both of these results are consistent with earlier single sphere outgrowth data. When 2.5% VEGF-A and 5% Sema3A spheres were placed on the same side of the SCG, there was not a significant increase in outgrowth towards the spheres compared to the non-sphere side of the SCG (Fig. 6D, fourth pair of bars). In contrast, when 5% VEGF-A and 2.5% Sema3A spheres were used, there was an approximately $18 \pm 6\%$ decrease in outgrowth towards the spheres compared to the non-sphere side of the SCG (Fig. 6D, fifth pair of bars). Our observation that the 2.5% VEGF/5% Sema3A combination did not elicit an inhibition of outgrowth is consistent with our previous data in which this concentration of Sema3A was noted not to affect outgrowth in single sphere co-cultures.

To confirm the role of Nrp1 signaling in regulating sympathetic neurite outgrowth, function-blocking Nrp1 antibodies were used in both SCG alone and SCG–vessel neurovascular co-cultures. In SCG alone cultures, concentrations as low as 500 ng/ml of Nrp1 antibody were able to decrease average axon length compared to control (Supplementary Figure 3D). To determine whether vascular-derived Nrp1 ligands are responsible for regulating patterns of sympathetic axon outgrowth in-vitro, femoral–SCG–carotid co-cultures were performed. At concentrations of 1 μg/ml and higher, Nrp1 antibodies

eliminated the increased outgrowth observed towards the femoral artery compared to the carotid (Supplementary Figure 3E). To determine whether VEGF-A/Nrp1 signaling mediated this effect, femoral–SCG single vessel cultures, concentrations of 1 μg/ml or higher were able to block the growth promoting effects of the femoral artery (data not shown). To determine whether Sema3A/Nrp1 signaling mediated the decrease in outgrowth towards carotid arteries, SCG–carotid co-cultures were performed and concentrations of 10 μg/ml or higher were able to block the growth inhibitory effects of the carotid artery (data not shown).

Finally, as neurite outgrowth and target innervation are inherently different processes, femoral and carotid arteries were co-cultured with whole SCG explants for five days to allow neurites to extend out to/past the vessel segments. Using phase microscopy, it appeared that neurites approached both vessels but only grew past the artery segment in carotid–SCG co-cultures (Fig. 7B). In femoral–SCG co-cultures, neurites grew to the vessel and did not appear to grow past the vessel segment (Fig. 7A). Using confocal microscopy, we imaged both neurovascular co-cultures to evaluate whether vessels were innervated by sympathetic axons following five days in culture. In carotid–SCG co-culture, tyrosine hydroxylase axons appeared to grow across the vessel as well as underneath but not wrap intimately around the vessel (Fig. 7D). In contrast, in femoral–SCG co-cultures, tyrosine hydroxylase positive axons wrapped extensively around the vessel and formed a dense meshwork of axons around the vessel, similar to what we observed in-vivo (Fig. 7C).

Additionally, when femoral–SCG co-cultures were double-labeled with anti tyrosine hydroxylase and synaptophysin, co-localization of a fraction of the synaptic varicosities was noted, consistent with sympathetic re-innervation (Figs. 7E, G). In contrast, in cultures of femoral artery segments alone, while synaptophysin puncta were still visible along the artery, no tyrosine hydroxylase immunofluorescence was observed, (Figs. 7F, H).

Discussion

Regional differences in vascular sympathetic innervation exist among arteries and veins (Fleming et al., 1989; Grasby et al., 1999; Griffith et al., 1982) suggesting that vascular-derived cues may drive axons to grow towards and ultimately innervate particular vessels. During development, axons extend growth cones that "interrogate" the environment for gradients of guidance cues that determine their direction of growth (Kolodkin, 1996; Tessier-Lavigne and Goodman, 1996). We developed an in-vitro 3D co-culture system to evaluate directed sympathetic neurite outgrowth towards both innervated and non-innervated arteries and to investigate the effects of endogenous attractive and repulsive gradients in determining patterns of neurite outgrowth. Our results demonstrate an increased axon outgrowth towards innervated arteries in-vivo, suggesting that these vessels produce chemoattractants and non-innervated arteries produce chemorepellants or different ratios of attractants and repellants that together may influence vascular innervation patterns. Our study identified VEGF-A and Semaphorin3A as chemoattractive and chemorepulsive cues respectively for sympathetic neurons. We have used our 3D co-culture to investigate the roles VEGF-A and Sema3A play in modulating selective sympathetic neuronal outgrowth towards vessels during development.

As axons extend towards their targets, they often travel along vessels, which express guidance factors including NT-3 and artemin (Belliveau et al., 1997; Damon, 2006; Damon et al., 2007). Sympathetic nerves that do interact with vessels do not form traditional synaptic terminals with vessels, but instead release neurotransmitter at periodic synaptic varicosities (see Fig. 1).

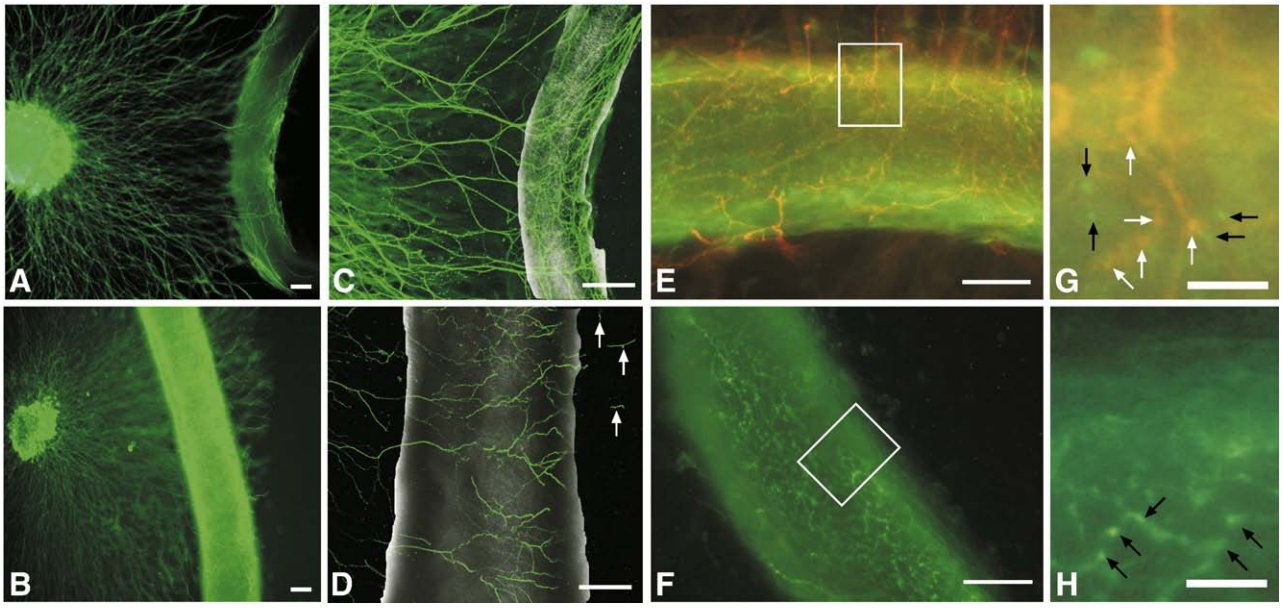

Fig. 7. Five-day neurovascular co-culture. (A, B) Fluorescent images of tyrosine hydroxylase sympathetic axons growing towards femoral (A) or carotid (B) artery segments for five days in co-culture. In femoral–SCG co-cultures axons grew out to, but did not pass the vessel in 6/7 co-cultures. In addition, the neurons appeared to make contact with and wrap around the vessel, forming a network parallel and perpendicular to the axis of the vessel similar to that seen in ex-vivo whole mount preparations (data not shown). Scale bar = 200 μm. (C, D) Confocal images of tyrosine hydroxylase immunofluorescence of SCG explants cultured with femoral (C) or carotid (D) artery segments for five days in 2.5 mg/ml collagen. Neurons comprising the femoral network were arranged both parallel and perpendicular to the vessel axis, investing the vessel, while neurons comprising the carotid network were arranged mainly perpendicular to the vessel axis with occasional axons migrating past the vessel segment (arrows) in 5/7 co-cultures. Scale bar = 200 μm. (E, F) Merged images of a five-day co-culture of a femoral artery segment with a SCG (E) and a segment of femoral artery cultured alone (F), illustrating synaptophysin staining (green fluorescence) and tyrosine hydroxylase staining (red fluorescence) of presynaptic varicosities, revealing co-localization of a portion of the varicosities suggestive of sympathetic re-innervation (orange fluorescence) in (E) and no detectable tyrosine hydroxylase staining in the mono-cultured femoral artery segment (F). Scale bar = 100 μm. (G, H) High power magnification insets of (E) and (F) illustrating specific synaptophysin labeled varicosities (green fluorescence denoted by black arrows) and synaptophysin/tyrosine hydroxylase co-labeled varicosities (orange fluorescence denoted by white arrows) in (G) and specific synaptophysin labeled varicosities (green fluorescence denoted by black arrows) in the mono-culture in(H). Scale bar = 25 μm.

Vessels produce guidance cues during development when innervation occurs. Previous studies in mouse have shown that sympathetic target innervation occurs between embryonic day 8 (E8) and postnatal day 20 (P20) (Glebova and Ginty, 2005). We observed significant increases in femoral innervation between P0–3, after which innervation densities are not different from adult. Thus we used P2 SCG, a time-point when significant vascular sympathetic innervation occurs and the animals are large enough to reproducibly dissect tissues for analysis.

In-vivo, axons follow complex gradients of long and short-range guidance cues and associate with extracellular matrix molecules in a three-dimensional environment (Kolodkin, 1996). A 3D in-vitro culture may better recapitulate the in-vivo complexity compared to traditional two-dimensional cultures. By incorporating both innervated and non-innervated vessels in culture with SCG we can maintain both attractive and repulsive gradients that together may determine patterns of axon outgrowth and target innervation in-vivo (Fig. 2). Our SCG explants cultured with single or both vessels showed increased outgrowth towards the femoral artery compared to the carotid (Figs. 2C and D). In addition, the carotid artery is capable of disrupting the increased axon outgrowth towards the femoral artery, suggesting that these arteries may produce chemoattractant and chemorepulsive cues whose ratios modulate differences in outgrowth and that the amount of carotid-derived chemorepellant may more directly influence patterns of neurite outgrowth (Fig. 2D).

While quantitative real-time PCR reveals that femoral arteries express more VEGF-A and the carotid expresses more Sema3A, Western blot analysis revealed that VEGF-A expression is not significantly different between the vessels, consistent with post-translational modifications affecting protein expression. In addition, sympathetic neurons express receptors for both guidance cues and there is no difference in localization of receptors in SCG cultured alone or in combination with innervated or non-innervated vessels. Given these findings, it is plausible that in-vivo vascular-derived VEGF-A and Sema3A may both modulate sympathetic axon outgrowth by differential signaling through Nrp-1, which can interact with VEGFR2 and Plexin1A, depending upon its counter ligand (Fig. 8).

To further evaluate the role of VEGF-A, we utilized high-expressing VEGF-A–LacZ mice, which ubiquitously express higher VEGF-A compared to wild-type littermates (Miquerol et al., 2000). By Western blot and qRT-PCR, VEGF-A (hi/+) femoral and carotid arteries express approximately 40% more VEGF-A. In VEGF-A (hi/+) mice there is a modest significant increase in femoral artery TH immunofluorescence, suggesting that VEGF-A level may play a role in determining sympathetic vascular innervation in-vivo. In-vitro 3D co-culture experiments using VEGF-A (hi/+) carotid artery segments with both wild-type and VEGF-A (hi/+) femoral segments suggest that increased carotid VEGF-A expression mutes normal carotid-derived growth inhibitory cues. In contrast, VEGF-A (hi/+) femoral artery segments were unable to increase axon length when used in-vitro with wild-type carotid arteries, suggesting a concentration-dependent behavior consistent with previous studies in which distinct concentration ranges of VEGF-A elicited specific cellular behaviors (Enciso et al., 2003; Pinter et al., 2001). This suggests that endogenous carotid-derived Sema3A may repress the outgrowth effects of VEGF-A, but increasing carotid VEGF-A expression decreases the Sema3A/Nrp1/Plexin1A signaling, allowing VEGF-A to promote enhanced outgrowth. Additionally, alginate spheres containing either 1.25% w/v or 2.5% w/v VEGF-A (Jay et al., 2008) induced significant increases in average axon length towards the VEGF-A gradient. However, increasing VEGF-A delivery by approximately 55% in-vitro by using 5% and 10% w/v VEGF-A alginate spheres did not elicit increased neurite outgrowth, suggesting again that cellular responsiveness to VEGF-A may fall within a narrow range (Enciso et al., 2003; Hallaq et al., 2004; Pinter et al., 2001; Rosoff et al., 2004). To ensure VEGF-A specificity, VEGF-A-neutralizing antibodies and a cell-specific VEGFR2 inhibitor were used to block sphere- and femoral artery-promoted outgrowth. Interestingly, while the inhibitor was able to decrease overall axon length in a dose-dependent manner, for a given concentration, the ratio of vessel/non-vessel average axon length was similar to control cultures. This may be due to an alternate signaling pathway activated by VEGF-A, such as via VEGFR1 signaling, which has been implicated in regulating sympathetic growth cone area (Marko and Damon, 2008). However, the use of VEGFR1 function-blocking antibodies was unable to decrease axon length or the increased outgrowth towards the femoral artery. Although these data are in contrast to previous studies (Marko and Damon, 2008) current studies may reflect species-specific differences or alterations in signaling between two- and three-dimensional cultures. In addition, while Nrp1-VEGFR1 interactions have been reported, the function of this complex is not known. In-vitro studies have demonstrated that Nrp1-VEGFR1 interactions inhibit VEGF-A binding to VEGFR1, thereby antagonizing VEGF-A signaling (Fuh et al., 2000). Alternatively, there may be other femoral-derived growth factors that play a role in regulating axon outgrowth. Multiple guidance cues may be present along an axon's trajectory towards its target and create a “passageway” through which the axon must navigate. In ours and previous studies, in the absence of VEGF-A or Sema3A signaling, significant baseline SCG outgrowth occurs, which supports this concept (Damon, 2006; Marko and Damon, 2008). Future evaluation of the expression profile of innervated vs. non-innervated vessels may help shed light on these additional factors.

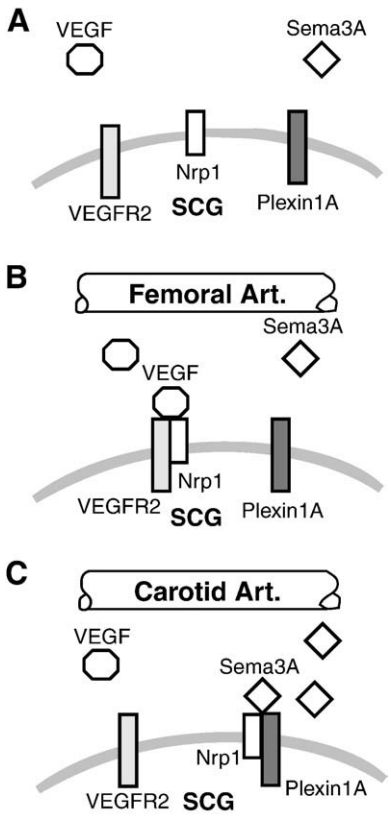

Fig. 8. Working model for the role of vascular-derived VEGF-A and Sema3A in modulating sympathetic axon outgrowth. (A) Schematic representing our model for the roles of VEGF-A and Sema3A in modulating sympathetic outgrowth. Both VEGF-A and Sema3A bind to Nrp1 and promote its association with a co-receptor, either VEGFR2 or PlexinA1. Both femoral and carotid arteries produce VEGF-A. (B) The femoral artery was noted to produce slightly more VEGF-A than the carotid artery. In the absence of chemorepulsive signals, femoral-derived VEGF-A can bind to Nrp1, which can then associate with VEGFR2, resulting in increased neurite outgrowth. (C) In contrast, the carotid artery was noted to produce approximately three times more Sema3A than the carotid artery, favoring Nrp1-bound Sema3A to associate with PlexinA1, resulting in blunted neurite outgrowth.

Previous studies have demonstrated a role for VEGF-A in promoting sympathetic neurite outgrowth (Marko and Damon, 2008). Our data revealed that while there is no significant difference in VEGF-A protein expression between vessels, the carotid expresses significantly more Sema3A compared to femoral arteries. This suggests that in-vivo the amount of Sema3A present in the environment may play a significant role in modulating sympathetic outgrowth patterns in these vessels as Sema3A has been implicated in sympathetic neuron outgrowth (Chen et al., 1998; Damon, 2006; Kawasaki et al., 2002; Suto et al., 2005). We conducted co-culture experiments using chimeric recombinant human Sema3A/Fc-encapsulated alginate spheres and as with VEGF-A, Sema3A spheres influenced neurite outgrowth in a dose-dependent manner with the largest reduction in outgrowth observed with a 2.5% w/v sphere. In addition, a similar loss of responsiveness at the highest Sema3A concentration was observed which supports previous reports of a narrow concentration range within which axons respond to chemical gradients (Rosoff et al., 2004).

To investigate whether gradients of VEGF-A and Sema3A combinatorially affect neurite outgrowth, dual sphere co-cultures were performed using VEGF-A and Sema3A/Fc spheres of equal concentrations within the responsive range (1.25% or 2.5% w/v) placed on opposite sides of the SCG. The results of these experiments were identical to single sphere co-cultures, suggesting that when these two molecules are present in similar concentrations (w/v) creating opposing gradients, neither molecule predominates. In additional experiments utilizing function-blocking antibodies specific to Nrp1 elicited decreased overall axon length in SCG explants, confirming that Nrp1 signaling plays a role in sympathetic axon outgrowth. In femoral–SCG–carotid co-cultures, blocking Nrp1 both decreased overall axon outgrowth and also eliminated the difference in outgrowth towards one vessel compared to another. This leads to the hypothesis that while VEGF signaling through VEGFR2 may play an important role in promoting increased axon outgrowth towards innervated vessels, Sema3a-Nrp1 signaling in dual vessel co-cultures may play the predominant role in determining overall patterns of outgrowth. In addition, Nrp1 antibodies blocked both the increase in outgrowth elicited by the femoral artery and the decrease in outgrowth elicited by the carotid artery in both single vessel co-cultures and femoral–SCG–carotid co-cultures, further suggesting that both VEGF-A/Nrp1 and Sema3A/Nrp1 signaling is at play in postnatal day 2 SCG. However, a higher concentration of antibody was required to reduce the blunting effect of the carotid artery, suggesting that there may be significantly different kinetics between VEGF-Nrp1 and Sema3A-Nrp1 signaling or possible that the carotid artery produces more Sema3A than was able to be neutralized by the antibody. Additional experiments investigating the affinity and binding kinetics of these two ligands for Nrp1 will be necessary to more definitively define the individual roles of VEGF-A and Sema3A in regulating sympathetic axon outgrowth.

In-vivo sympathetic nerves may encounter overlapping gradients of guidance cues. Combinations of such gradients may be necessary for sympathetic nerves to properly find and innervate final targets. Previous studies have demonstrated that the balance of VEGF-A and Sema3A may influence particular cellular responses (Vieira et al., 2007; Schwarz et al., 2004). Our data shows that both the femoral and carotid arteries express significant VEGF-A, but only the carotid expresses significant Sema3A, suggesting that sympathetic growth cones may detect the higher Sema3A levels within the VEGF-A gradient. Hence, the increased Sema3A molecules may result in increased Sema3A–Nrp1 binding, eliciting increased Nrp1–Plexin interaction and intracellular signaling, resulting in decreased axon outgrowth. To evaluate the effect of overlapping gradients, we placed both VEGF-A and Sema3A spheres on the same side of the SCG and measured neurite outgrowth. Our finding that increases in Sema3A concentration block the growth promoting effects of VEGF-A suggests that the presence of increasing concentrations of Sema3A may be able to elicit increased Sema3A–Nrp1–PlexinA1 and thus may be a determining factor that limits sympathetic neurite outgrowth when both molecules are present in the extracellular environment.

Our data suggests that vascular-derived VEGF-A and Sema3A influence sympathetic outgrowth in-vitro and together may in part determine patterns of vascular sympathetic outgrowth in-vivo during development. To evaluate whether femoral and carotid-derived cues not only promote variations in axon outgrowth but differential innervation of vessels, we performed five-day neurovascular co-cultures to determine whether axons would innervate femoral and/or carotid arteries. While axons extended to both vessels, in carotid arteries axons grew past the vessel and appeared to grow across the vessel surface. In contrast, sympathetic axons rarely grew past femoral artery segments and instead formed an elaborate mesh of axons around the vessel, similar to what we observed ex-vivo, suggesting that these axons were potentially re-innervating the vessel. Further studies would allow us to determine whether these axons made functional contacts with the vessels and will shed light on the molecules responsible for this differential response.

Our data demonstrates that while both innervated and non-innervated vessels produce chemoattractive molecules (VEGF-A), non-innervated vessels may produce significantly more chemorepulsive factors (Sema3A). Thus, gradients of guidance cues may work in combination to direct outgrowth and ultimate innervation patterns. Increased carotid Sema3A expression may blunt the effect of VEGF-A, therefore playing a predominant role in regulating sympathetic axon outgrowth when both molecules are present (Fig. 8). It is also likely that other signaling pathways are involved in-vivo as nearby cells or tissues likely produce additional cues that direct axonal growth cones away from non-innervated vessels or produce alternate cues that strengthen the chemorepulsive cues that originate from the vessels themselves.

Acknowledgments

We would like to thank Carlos Hernandez for his technical assistance, Erin Lavik for the use of her microscope and Michael Schwartz for the generous use of the Neurolucida system. Thank you to George Tellides and Larry Lo for supplying us with the EYFP mice and for their assistance in isolating vascular smooth muscle cells. Thanks also to Sandra Canosa for her critical reading of this manuscript and to Tom Ardito for his assistance with confocal microscopy. This work was supported by USPHS grants R37-HL28373, RO1-HL51018 and the Reed Foundation to JAM, F31NS062581 to JBL, NIH HL085416 for SMJ, W. Mark Saltzman (PI), NIH-HL056786 to SSS. The VEGF-A used in these studies was generously supplied by the NCI.

Appendix A. Supplementary data

Supplementary data associated with this article can be found, in the online version, at doi:10.1016/j.ydbio.2009.07.023.

References

Adams, R.H., Wilkinson, G.A., Weiss, C., Diella, F., Gale, N.W., Deutsch, U., Risau, W., Klein, R., 1999. Roles of ephrinB ligands and EphB receptors in cardiovascular development: demarcation of arterial/venous domains, vascular morphogenesis, and sprouting angiogenesis. Genes Dev. 13, 295–306.

Appleton, B.A., Wu, P., Maloney, J., Yin, J., Liang, W.C., Stawicki, S., Mortara, K., Bowman, K.K., Elliott, J.M., Desmarais, W., Bazan, J.F., Bagri, A., Tessier-Lavigne, M., Koch, A.W., Wu, Y., Watts, R.J., Wiesmann, C., 2007. Structural studies of neuropilin/antibody complexes provide insights into semaphorin and VEGF binding. EMBO J. 26, 4902–4912.

Bagnard, D., Vaillant, C., Khuth, S.T., Dufay, N., Lohrum, M., Puschel, A.W., Belin, M.F., Bolz, J, Thomasset, N., 2001. Semaphorin 3A-vascular endothelial growth factor-165 balance mediates migration and apoptosis of neural progenitor cells by the recruitment of shared receptor. J. Neurosci. 21, 3332–3341.

Belliveau, D.J., Krivko, I., Kohn, J., Lachance, C., Pozniak, C., Rusakov, D., Kaplan, D., Miller,

F.D., 1997. NGF and neurotrophin-3 both activate TrkA on sympathetic neurons but differentially regulate survival and neuritogenesis. J. Cell Biol. 136, 375–388.
Birch, D.J., Turmaine, M., Boulos, P.B., Burnstock, G., 2008. Sympathetic innervation of human mesenteric artery and vein. J. Vasc. Res. 45, 323–332.
Carmeliet, P., 2003. Blood vessels and nerves: common signals, pathways and diseases. Nat. Rev. Genet. 4, 710–720.
Chen, H, He, Z, Bagri, A, Tessier-Lavigne, M., 1998. Semaphorin–neuropilin interactions underlying sympathetic axon responses to class III semaphorins. Neuron 6, 1283–1290.
Cheng, L., Jia, H., Lohr, M., Bagherzadeh, A., Holmes, D.I., Selwood, D., Zachary, I., 2004. Anti-chemorepulsive effects of vascular endothelial growth factor and placental growth factor-2 in dorsal root ganglion neurons are mediated via neuropilin-1 and cyclooxygenase-derived prostanoid production. J. Biol. Chem. 279, 30654–30661.
Damon, D.H., 2006. Vascular endothelial-derived semaphorin 3 inhibits sympathetic axon growth. Am. J. Physiol. Heart Circ. Physiol. 290, H1220–H1225.
Damon, D.H., Teriele, J.A., Marko, S.B., 2007. Vascular-derived artemin: a determinant of vascular sympathetic innervation? Am. J. Physiol. Heart Circ. Physiol. 293, H266–H273.
Enciso, J.M., Gratzinger, D., Camenisch, T.D., Canosa, S., Pinter, E., Madri, J.A., 2003. Elevated glucose inhibits VEGF-A-mediated endocardial cushion formation: modulation by PECAM-1 and MMP-2. J. Cell Biol. 160, 605–615.
Enomoto, H., Crawford, P.A., Gorodinsky, A., Heuckeroth, R.O., Johnson Jr., E.M., Milbrandt, J., 2001. RET signaling is essential for migration, axonal growth and axon guidance of developing sympathetic neurons. Development 128, 3963–3974.
Fan, J., Raper, J.A., 1995. Localized collapsing cues can steer growth cones without inducing their full collapse. Neuron 14, 263–274.
Fleming, B.P., Gibbins, I.L., Morris, J.L., Gannon, B.J., 1989. Noradrenergic and peptidergic innervation of the extrinsic vessels and microcirculation of the rat cremaster muscle. Microvasc. Res. 38, 255–268.
Fuh, G., Garcia, C.K., de Vos, A.M., 2000. The interaction of neuropilin-1 with vascular endothelial growth factor and its receptor flt-1. J. Biol. Chem. 275, 26690–26695.
Geretti, E., Shimizu, A., Klagsbrun, M., 2008. Neuropilin structure governs VEGF and semaphorin binding and regulates angiogenesis. Angiogenesis 11, 31–39.
Glebova, N.O., Ginty, D.D., 2004. Heterogeneous requirement of NGF for sympathetic target innervation in vivo. J. Neurosci. 24, 743–751.
Glebova, N.O., Ginty, D.D., 2005. Growth and survival signals controlling sympathetic nervous system development. Annu. Rev. Neurosci. 28, 191–222.
Grasby, D.J., Morris, J.L., Segal, S.S., 1999. Heterogeneity of vascular innervation in hamster cheek pouch and retractor muscle. J. Vasc. Res. 36, 465–476.
Griffith, S.G., Crowe, R., Lincoln, J., Haven, A.J., Burnstock, G., 1982. Regional differences in the density of perivascular nerves and varicosities, noradrenaline content and responses to nerve stimulation in the rabbit ear artery. Blood Vessels 19, 41–52.
Hallaq, H., Pinter, E., Enciso, J., McGrath, J., Zeiss, C., Brueckner, M., Madri, J., Jacobs, H.C., Wilson, C.M., Vasavada, H., Jiang, X., Bogue, C.W., 2004. A null mutation of Hhex results in abnormal cardiac development, defective vasculogenesis and elevated Vegfa levels. Development 131, 5197–5209.
He, Z., Tessier-Lavigne, M., 1997. Neuropilin is a receptor for the axonal chemorepellent semaphorin III. Cell 90, 739–751.
Herzog, Y., Kalcheim, C., Kahane, N., Reshef, R., Neufeld, G., 2001. Differential expression of neuropilin-1 and neuropilin-2 in arteries and veins. Mech. Dev. 109, 115–119.
Honma, Y., Araki, T., Gianino, S., Bruce, A., Heuckeroth, R., Johnson, E., Milbrandt, J., 2002. Artemin is a vascular-derived neurotropic factor for developing sympathetic neurons. Neuron 35, 267–282.
Jay, S.M., Shepherd, B.R., Bertram, J.P., Pober, J.S., Saltzman, W.M., 2008. Engineering of multifunctional gels integrating highly efficient growth factor delivery with endothelial cell transplantation. Faseb J. 22, 2949–2956.
Kawasaki, T, Bekku, Y, Suto, F, Kitsukawa, T, Taniguchi, M, Nagatsu, I, Nagatsu, T, Itoh, K, Yagi, T, Fujisawa, H., 2002. Requirement of neuropilin 1-mediated Sema3A signals in patterning of the sympathetic nervous system. Development 3, 671–680.
Kitsukawa, T., Shimizu, M., Sanbo, M., Hirata, T., Taniguchi, M., Bekku, Y., Yagi, T., Fujisawa, H., 1997. Neuropilin–semaphorin III/D-mediated chemorepulsive signals play a crucial role in peripheral nerve projection in mice. Neuron 19, 995–1005.
Kolodkin, A.L., 1996. Growth cones and the cues that repel them. Trends Neurosci. 19, 507–513.
Kolodkin, A.L., Levengood, D.V., Rowe, E.G., Tai, Y.T., Giger, R.J., Ginty, D.D., 1997. Neuropilin is a semaphorin III receptor. Cell 90, 753–762.
Kuruvilla, R., Zweifel, L.S., Glebova, N.O., Lonze, B.E., Valdez, G., Ye, H., Ginty, D.D., 2004. A neurotrophin signaling cascade coordinates sympathetic neuron development through differential control of TrkA trafficking and retrograde signaling. Cell 118, 243–255.
Li, Q., Michaud, M., Stewart, W., Schwartz, M., Madri, J.A., 2007. Modeling the neurovascular niche: murine strain differences mimic the range of responses to chronic hypoxia in the premature newborn. J. Neurosci. Res. 86, 1227–1242.
Lin, G., Chen, K.C., Hsieh, P.S., Yeh, C.H., Lue, T.F., Lin, C.S., 2003. Neurotrophic effects of vascular endothelial growth factor and neurotrophins on cultured major pelvic ganglia. B.J.U. Int. 92, 631–635.
Livak, K.J., Schmittgen, T.D., 2001. Analysis of relative gene expression data using real-time quantitative PCR and the 2(-Delta Delta C(T)) Method. Methods 25, 402–408.
Looft-Wilson, R.C., Haug, S.J., Neufer, P.D., Segal, S.S., 2004. Independence of connexin expression and vasomotor conduction from sympathetic innervation in hamster feed arteries. Microcirculation 11, 397–408.
Madri, J.A., Pratt, B.M., Tucker, A.M., 1988. Phenotypic modulation of endothelial cells by transforming growth factor-beta depends upon the composition and organization of the extracellular matrix. J. Cell Biol. 106, 1375–1384.
Marko, S.B., Damon, D.H., 2008. VEGF promotes vascular sympathetic innervation. Am. J. Physiol. Heart Circ. Physiol. 294, H2646–H2652.
Miao, H.Q., Soker, S., Feiner, L., Alonso, J.L., Raper, J.A., Klagsbrun, M., 1999. Neuropilin-1 mediates collapsin-1/semaphorin III inhibition of endothelial cell motility: functional competition of collapsin-1 and vascular endothelial growth factor-165. J. Cell Biol. 146, 233–242.
Miquerol, L., Gertsenstein, M., Harpal, K., Rossant, J., Nagy, A., 1999. Multiple developmental roles of VEGF suggested by a LacZ-tagged allele. Dev. Biol. 212, 307–322.
Miquerol, L., Langille, B.L., Nagy, A., 2000. Embryonic development is disrupted by modest increases in vascular endothelial growth factor gene expression. Development 18, 3941–3946.
Nordal, R.A., Nagy, A., Pintilie, M., Wong, C.S., 2004. Hypoxia and hypoxia-inducible factor-1 target genes in central nervous system radiation injury: a role for vascular endothelial growth factor. Clin. Cancer Res. 10, 3342–3353.
Ogunshola, O.O., Antic, A., Donoghue, M.J., Fan, S.Y., Kim, H., Stewart, W.B., Madri, J.A., Ment, L.R., 2002. Paracrine and autocrine functions of neuronal vascular endothelial growth factor (VEGF) in the central nervous system. J. Biol. Chem. 277, 11410–11415.
Pinter, E., Haigh, J., Nagy, A., Madri, J.A., 2001. Hyperglycemia-induced vasculopathy in the murine conceptus is mediated via reductions of VEGF-A expression and VEGF receptor activation. Am. J. Pathol. 158, 1199–1206.
Rosenstein, J.M., Krum, J.M., 2004. New roles for VEGF in nervous tissue—beyond blood vessels. Exp. Neurol. 187, 246–253.
Rosoff, W.J., Urbach, J.S., Esrick, M.A., McAllister, R.G., Richards, L.J., Goodhill, G.J., 2004. A new chemotaxis assay shows the extreme sensitivity of axons to molecular gradients. Nat. Neurosci. 7, 678–682.
Ruffolo Jr., R.R., Nichols, A.J., Stadel, J.M., Hieble, J.P., 1991. Structure and function of alpha-adrenoceptors. Pharmacol. Rev. 43, 475–505.
Schwamborn, J.C., Fiore, R., Bagnard, D., Kappler, J., Kaltschmidt, C., Puschel, A.W., 2004. Semaphorin 3A stimulates neurite extension and regulates gene expression in PC12 cells. J. Biol. Chem. 279, 30923–30926.
Schwarz, Q., Gu, C., Fujisawa, H., Sabelko, K., Gertsenstein, M., Nagy, A., Taniguchi, M., Kolodkin, A.L., Ginty, D.D., Shima, D.T., Ruhrberg, C., 2004. Vascular endothelial growth factor controls neuronal migration and cooperates with Sema3A to pattern distinct compartments of the facial nerve. Genes Dev. 18, 2822–2834.
Smith, M.K., Peters, M.C., Richardson, T.P., Garbern, J.C., Mooney, D.J., 2004. Locally enhanced angiogenesis promotes transplanted cell survival. Tissue Eng. 10, 63–71.
Soker, S., Takashima, S., Miao, H.Q., Neufeld, G., Klagsbrun, M., 1998. Neuropilin-1 is expressed by endothelial and tumor cells as an isoform-specific receptor for vascular endothelial growth factor. Cell 92, 735–745.
Sondell, M., Kanje, M., 2001. Postnatal expression of VEGF and its receptor flk-1 in peripheral ganglia. Neuroreport 12, 105–108.
Sondell, M., Lundborg, G., Kanje, M., 1999. Vascular endothelial growth factor has neurotrophic activity and stimulates axonal outgrowth, enhancing cell survival and Schwann cell proliferation in the peripheral nervous system. J. Neurosci. 19, 5731–5740.
Sondell, M., Sundler, F., Kanje, M., 2000. Vascular endothelial growth factor is a neurotrophic factor which stimulates axonal outgrowth through the flk-1 receptor. Eur. J. Neurosci. 12, 4243–4254.
Spandidos, A., Wang, X., Wang, H, Dragnev, S., Thurber, T., Seed, B., 2008. A comprehensive collection of experimentally validated primers for Polymerase Chain Reaction quantitation of murine transcript abundance. BMC Genomics 9, 633.
Srinivas, S., Watanabe, T., Lin, C.S., William, C.M., Tanabe, Y., Jessell, T.M., Costantini, F., 2001. Cre reporter strains produced by targeted insertion of EYFP and ECFP into the ROSA26 locus. BMC Dev. Biol. 1 (4).
Storkebaum, E., Lambrechts, D., Dewerchin, M., Moreno-Murciano, M.P., Appelmans, S., Oh, H., Van Damme, P., Rutten, B., Man, W.Y., De Mol, M., Wyns, S., Manka, D., Vermeulen, K., Van Den Bosch, L., Mertens, N., Schmitz, C., Robberecht, W., Conway, E.M., Collen, D., Moons, L., Carmeliet, P., 2005. Treatment of motor neuron degeneration by intracerebroventricular delivery of VEGF in a rat model of ALS. Nat. Neurosci. 8, 85–92.
Sun, L., Tran, N., Tang, F., App, H., Hirth, P., McMahon, G., Tang, C., 1988. Synthesis and biological evaluations of 3-substituted indolin-2-ones: a novel class of tyrosine kinase inhibitors that exhibit selectivity toward particular receptor tyrosine kinases. J. Med. Chem. 41, 2588–2603.
Suto, F., Ito, K., Uemura, M., Shimizu, M., Shinkawa, Y., Sanbo, M., Shinoda, T., Tsuboi, M., Takashima, S., Yagi, T., Fujisawa, H., 2005. Plexin-a4 mediates axon-repulsive activities of both secreted and transmembrane semaphorins and plays roles in nerve fiber guidance. J. Neurosci. 14, 3628–3637.
Tan, A.Y., Chen, P.S., Chen, L.S., Fishbein, M.C., 2007. Autonomic nerves in pulmonary veins. Heart Rhythm (3 Suppl), S57–S60.
Tessier-Lavigne, M., Goodman, C.S., 1996. The molecular biology of axon guidance. Science 274, 1123–1133.
Vieira, J.M., Schwarz, Q., Ruhrberg, C., 2007. Selective requirements for NRP1 ligands during neurovascular patterning. Development 134, 1833–1843.
Wang, X., Seed, B., 2003. A PCR primer bank for quantitative gene expression analysis. Nucleic Acids Res. 31, e154.
Wingerd, K.L., Goodman, N.L., Tresser, J.W., Smail, M.M., Leu, S.T., Rohan, S.J., Pring, J.L., Jackson, D.Y., Clegg, D.O., 2002. Alpha 4 integrins and vascular cell adhesion molecule-1 play a role in sympathetic innervation of the heart. J. Neurosci. 22, 10772–10780.
Xu, X., Francis, R., Wei, C.J., Linask, K.L., Lo, C.W., 2006. Connexin 43-mediated modulation of polarized cell movement and the directional migration of cardiac neural crest cells. Development 133, 3629–3639.
Young, H.M., Anderson, R.B., Anderson, C.R., 2004. Guidance cues involved in the development of the peripheral autonomic nervous system. Auton. Neurosci. 112, 1–14.